MASTER THESIS

ADVANCED RANGING TECHNIQUES IN UWB BASED LOCALIZATION

Merhawi Tecle Berhe

DEPARTMENT OF ELECTRICAL ENGINEERING
TELECOMMUNICATION ENGINEERING GROUP

EXAMINATION COMMITTEE
Prof. dr. W. G. Scanlon
Dr. ir. M. J. Bentum
Dr. ir. A. Meijerink
Dr. ir. G. J. Heijenk
Y. Kılıç, M.Sc.

DOCUMENT NUMBER
-

UNIVERSITY OF TWENTE.

FEB. 23,2012

Acknowledgment

First of all, I would like to thank God for giving me the strength not only to complete my MSc but for seeing me though my difficulties and hard times. If it wasn't for you, doing my MSc would have been one of my unfulfilled dreams. Thank you Jesus, for your blessing!

I would like to pass my heartfelt regards to my family, no words would be enough to expressing their deeds. Warren Buffet once said, the secrete behind his success is that he won the genetic lottery. I can't agree more. Thank you dad, mam and the three musketeers-Yoni, Meri and Kisun.

I consider myself blessed to have two families in my life. Baba Teka, mama Nigstey and you lovely family, you were there during my dark days and you brought me to light. You have given me the best gift that one person can give and I can't thank you enough for that. May the lord bless you abundantly.

Rahela, though far away, you being in my life has made everything more interesting and worth doing. You have made the long two years seem like two months. Thank you for being just a call away.

When people asking me why I did my thesis with the TE group, I would sarcastically say I like the people up there. I really meant it. My gratitude goes to everyone in the group, but especially to my supervisors Yakup, Arjan and Mark. Yakup, thank you for being there whenever I needed you. Arjan, I have enjoyed the quite length discussion we have had during the last few months.

I have never seen a person that critical and detailed. I am sure I am better person as the result of those discussions. Mark, though we haven't met much during the thesis, your humors always made my day.

My enthusiasm to do MSc has come to being as a result of the Universtity of Twente scholarship (UTS). I wouldn't be able to purse my study if it wasn't for this scholarship. Thus, I would like to thank everyone involved with the scholarship, especially, EEMC internationalizing coordinator (Dr. Maarten Korsten), the international office and the visa office.

Acknowledgment would be incomplete without mentioning the contributions of my friends. Anbes, thank you for everything. My study would have been difficult if not impossible without your support. Misgates, you were there during my last days of study, where things were a bit stressful. Thank you for having the patience to listen. Moss 'Koratu', thank you for teaching what it means to be optimistic and positive minded practically. Zerit, you brought fun to the group, something that was dearly needed in those two years.

Summary

In the last decade or so, indoor positioning systems have been gaining a lot of attention. Tracking objects and people, entertainment and gaming, health care applications, military and first responders, environment monitoring and treatment are some of the areas that can benefit from such a system.

Ultra wideband (UWB) signals are opted as the optimal solution in indoor positioning systems. This has to do with the unique characteristics of UWB signals. Because UWB signals have large bandwidth, they are able to resolve many multipaths. This enables accurate detection of the direct path which gives information regarding the range of the target node. When used with UWB signals, time of arrival ranging techniques can provide us with cm level accuracy in line of sight (LOS) situations. However, this technique has some serious challenges:

- In low signal to noise ratio (SNR) situations, the noise could obscure the information signal. In such cases, it might be impossible to detect the first peak that corresponds to the direct path. Thus, in such cases, there is a need to suppress the noise without degrading the information signal.

- In case of obstructed line of sight (OLOS) or non-line of sight (NLOS) scenarios, due to the presence of the obstacles between the target and the reference node, the direct path is either delayed or it is completely absent at the receiver. This results in a positively biased

distance estimation. In such case, there is a need to estimate the bias introduced and ultimately mitigate it.

In light of those challenges, this thesis can be divided in three parts. The first part deals with improving the SNR in ToA ranging systems. In this case, wavelet based de-noising techniques are used. The second part deals with LOS and NLOS identification. Characteristic features are extracted from the received signal and a relation is established between those features and the scenario. Classification algorithms are then developed using machine learning techniques in identifying if a node is in LOS or not. The third part of the thesis deals with estimating the range error in NLOS situations and mitigating it. In doing so, characteristic features are analyzed. An investigation is done on which features are more correlated to the error in ranging. Using regression algorithms, a relation is established between the error in ranging and the most promising features. Along with the IEEE 802.15.4a channel model, 200 actual measurements made in an indoor office are used in validating and assessing the various techniques used in this thesis.

Wavelet de-noising improved the detectability of the signal and ultimately the first peak under low SNRs. Depending on the SNR, the number of measurements within 1 m in range error increased significantly in the case of LOS. In the NLOS cases, similar significant improvements where achieved in the number of measurements that are within 10 m in range error. By using two features, namely kurtosis and number of significant paths, the classification algorithm was 100% successful. The success rate did not depend on the type or complexity of the classifier used. The identification technique is affected adversely by both noise and wavelet de-noising. Regarding the range error in NLOS, by using SVM classifiers along with the global peak, mean excess delay and range estimate, the maximum range error decreased from about 12.5 m to 11 m, while the root mean square error was reduced from 6.7 m to 2.8 m. However, no significant improvement was obtained with the number of measurements that are within 1 m in range error.

In conclusion, while improving the number of measurements that can be used for localization, wavelet de-noising has reduced the accuracy of the measurements. In this case, there is a trade off. The performance of channel identification is degraded by noise and also by de-noising. Thus, a technique that is SNR dependent, could improve the performance. Regression, while decreasing the RMSE, has not proven to be of great value when it comes to the errors that are less than 1 m. However, this could be a pre-mature conclusion, since regression depends on the number of training samples. Hence, our procedure should be repeated with an increased number of measurements and conclusive analysis should be made from that.

The results of this thesis are based on a limited number of measurements (200), of which 40 are in LOS and 160 are in NLOS.

Contents

Chapter 1

INTRODUCTION

This chapter introduces the field of sensor networks and localization. The different ranging techniques along with their merits and challenges will be discussed. The motivation and driving force for this thesis are also addressed in this chapter.

1.1 Indoor positioning systems

In recent years, localization based applications have been gaining great interest. These application could extend from public usage to military and safety activities. Typical scenarios include but are obviously not limited to inventory and equipment tracking in warehouses and manufacturing floors, patient and medical equipment tracking in hospitals, and first responder and soldier tracking for fire fighters and battle field troops [1]. Other applications of localization include wireless sensor networks where the localization is part of a bigger task like environmental sensing and industrial monitoring, water/waste treatment control.

Broadly speaking, there are three types of positioning techniques namely, scene analysis, proximity and geometrical localization. In scene analysis based localization, features (fingerprints) of a scene are collected and then estimation of the location of an object is done by matching online measurements with the closest a prior location fingerprints [3]. This requires prior knowledge of the environment. Moreover, a large database is needed to store initial location fingerprints, making it less favorable for sensor networks.

Proximity localization is another technique that provides us with a relative position. A number of anchor sensors with known position are used, and the position of the target node is determined with respect to those anchor nodes. If the target node is detected by one of the reference nodes, then it is considered to be collocated with that reference node. This technique requires a dense sensor (anchor) environment to have good accuracy.

Geometrical localization is generally composed of two steps: ranging and localization, see Figure 1.1. The ranging process is an action of estimating the distance [2]. In special cases like in angle of arrival (AoA) techniques, it could also mean finding the direction or angle between two nodes with respect to a given reference. The most common ranging techniques are time of arrival (ToA), angle of arrival (AoA), received signal strength information (RSSI), time difference of arrival (TDoA) and two way time of flight (TW-TOF) techniques. Those techniques are discussed in the forthcoming sections. Localization is the mechanism of finding the exact location of a given node by utilizing the range estimates.

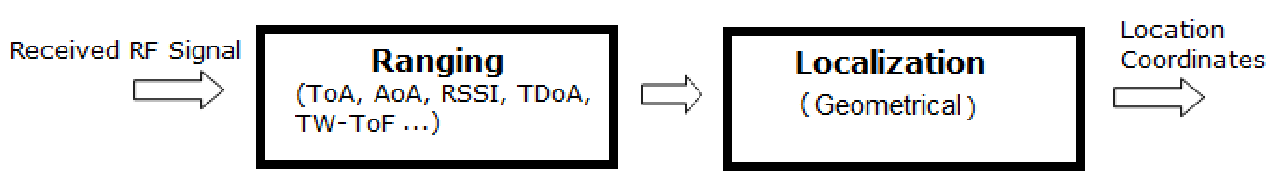

Figure 1.1: Functional block diagram of a wireless positioning system using geometric localization

Geometric properties are used to estimate the target location in geometric localization. This technique is accurate and simple. Thus, this technique is preferred over the previous ones. Details of geometric localization technique are discussed in the coming section.

1.1.1 Geometrical localization techniques

To do geometrical localization, anchor nodes are required. Geometrical techniques can be divided into two namely *triangulation and trilateration*. Triangulation needs angle information in determining the location of a target node. In order to have angle information, there is a need for an array of antennas or a directional antenna, which makes it complex and less cost effective.

Trilateration, on the other hand, is simple and cost effective. This technique uses distance information; see Figure 1.2a. The distance estimate of a target node from an anchor node roughly defines the position of the sensor on a circle whose center is the anchor node and radius is the estimated distance. In order to find the exact point on the circle, two other distance estimates, which would give another two circles, are required. The intersection of these three circles will determine the exact position of the target node.

Thus, to find the location of a sensor in a two dimensional space, we need to have three range estimates. Each range estimate is made by one of the approaches mentioned in the coming section.

The final positioning accuracy of trilateration greatly depends on the accuracy of each range estimate and the positions of the anchor nodes. An error in the range estimate would give an error in the estimated location of the sensor. For instance, in Figure 1.2b, the three circles do not intersect at a single point. This is created due to an error in one or more of the range estimates. In this case, the target node is likely to be located somewhere close to the dark colored region.

1.1.2 Ranging techniques

The last decade has seen a number of research efforts in the field of ranging. Various techniques and algorithms have been developed to come up with a more accurate and precise ranging

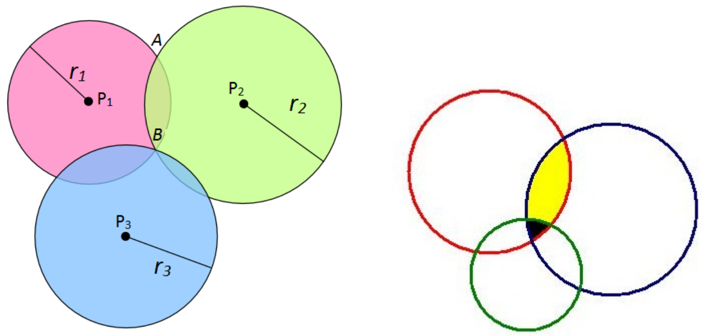

(a) Trilateration

(b) Trilateration with an error in at least one of the range estimates

Figure 1.2: Trilateration with (b) and without (a) ranging error

estimate. A brief overview of the common methodologies is given below.

Received signal strength information

RSSI makes use of the received signal energy for estimating the distance. This approach relates the attenuation in the signal energy with distance. However, this requires prior knowledge of the environment and the path loss exponent regarded for that environment.

If we have the knowledge of the path loss of the environment and the transmitted power, then, by measuring the strength of the received signal we can estimate the distance between the transmitting and receiving nodes.

RSSI avoids the need for synchronization [16]. This is the main advantage of RSSI. Therefore, this technique is regarded as simple and less power consuming. However, the inaccuracies present in estimating the shadowing and fading of the environment and in estimating the RSS lead to a large ranging error. Moreover, the accuracy of the method depends on the distance between the sensors, making it appropriate for short distances only [13].

Time of arrival

In the ToA technique, the receiver measures the travel time, and, accordingly, estimates the distance. It is simple, and, therefore, cost effective. The distance estimate is given by the estimated time of flight multiplied by the velocity of the signal, which is the speed of light for electromagnetic waves.

This mechanism is highly accurate when there is a direct path i.e. line of sight (LOS) between the nodes. However, its accuracy is degraded when the nodes are not in line of sight, i.e. when the nodes are either in obstructed line of sight (OLOS) or non-line of sight (NLOS). This is because of the additional time bias introduced by the obstacles, as is explained in Section 1.2.2.

The ToA technique requires very precise knowledge of the transmission start time, and must ensure synchronization between the nodes involved. TW-ToF, can be used in order to avoid the need for synchronization. In this case, a round trip time is used to estimate the distance between the nodes. TDOA is another technique that avoids the need for synchronization between the target and anchor nodes. Details of TW-ToF and TDOA are presented in [3].

While traditionally, sampling rates in the order of several GHz are required, it is proposed in [19] that only tens of MHz sampling rates can provide us with a reasonable accuracy.

1.2 Ultra-wideband ranging

1.2.1 Ultra-wideband and its silent features

UWB signals are characterized by a bandwidth which is either greater than 500 MHz or exceeding 20% of the center frequency of radiation [7]. This wide spectrum is often implemented by generating waveforms with short pulses, in the order of nanoseconds. Ultra-wideband signals were regulated by the FCC in 2002 and are becoming the most viable solution for indoor positioning. One of the standards for wireless personal area networks with UWB in the physical layer is the IEEE 802.15.4a standard, where UWB is used in the range of $3-10$ GHz [7], according to the FCC regulation.

Because of the very small pulse duration, using UWB improves the multipath resolvability. Multipath resolvability is defined as the number of paths that can be separated by a receiver [9]. Thus, one of the advantages of UWB is its ability to distinguish multipaths. Because of the lower frequency components, UWB signals can penetrate obstacles reaching to objects that are hidden or shadowed by certain materials.

It is mainly those two advantages (multipath resolvability and penetration through obstacles) that make UWB the most appropriate solution for indoor localization and ranging [10].

Additionally, UWB signals can be transmitted without a carrier and therefore are known as *carrierless* signals [11], giving rise to lower cost, more power efficient receivers, and less complex front end design. This makes them suitable for sensor technology. According to the FCC, in order to avoid any interference that could be caused by UWB to other currently present technologies, the maximum transmission power is subject to -41 dBm/MHz, limiting its application to moderate data rates or short range communication.

Theoretically, UWB can offer sub-centimeter level ranging accuracy with a very high precision.

1.2.2 Major sources of error in UWB ranging

Indoor environments are subject to obstacles and reflectors. As discussed in the previous section, there are different approaches that can be employed in range estimation. From simplicity perspective, RSSI is the least complex method. However, this technique is environment dependent, as there is a need to know the path loss exponent. Moreover, the accuracy of RSSI is distance dependent: with increasing distance its accuracy will degrade. This technique also fails short of fully utilizing the specific advantages of UWB.

On the other hand, ToA makes use of the unique advantages of UWB signals. (Details are presented in Chapter 2.) In addition, the accuracy of ToA ranging depends on the bandwidth and the SNR of the signal used. Hence, using UWB with ToA will give more accurate results. Therefore, in this thesis, the ranging issues will be addressed from a ToA prospective.

One of the most prominent and highly addressed problems in ToA ranging is the absence of LOS. In indoor offices, for instance, it is rare to have a direct line of sight (LOS) between the transmitter and receiver. There will be objects that will block the transmitter from the receiver or vise verse. This leads to two additional scenarios- OLOS and NLOS situations, as illustrated in Figure 1.3. In the OLOS situation, an obstacle is present between the transmitter and receiver. The transmitted signal, however, is able to penetrate this obstacle and reach the receiver. Because of its permittivity, the obstacle will slow down the transmitted signal, causing an additional bias in time. Moreover, the first peak, signaling the direct path, could also be attenuated so much that we may not be able to distinguish it from the background noise. This could lead to considering later multipaths as the first peak, leading to an erroneous range estimate. This phenomena is discussed in detail in the coming chapters.

In the case of NLOS the obstacle present between the transmitter and receiver does not allow the signal wave to travel across. This could happen if, for instance, the obstacle is a metal sheet or aluminum cabinet. In this case, the received signal only contains signals that have been reflected by objects nearby. There is no direct path or delayed version of the direct paths. This results in assuming the earliest reflections as the direct path, resulting in an erroneous range estimate.

As such, in both above cases (OLOS/NLOS), it becomes necessary to find the positive time bias incurred by the obstacles in the environment.

In the case of LOS, the error is due to mainly the noise and possible synchronization errors. Nevertheless, it is possible to have cm level accuracies with LOS situations. However, in the case of OLOS/NLOS, the accuracy is highly degraded due to the time bias, making ranging error

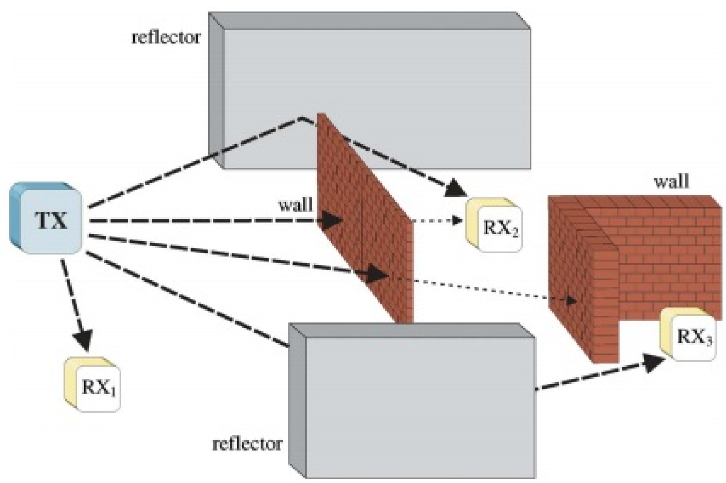

Figure 1.3: The three possible situations, Receiver 1 (RX_1) is in LOS, while Receiver 2 (RX_2) is in OLOS and Receiver 3 (RX_3) is in NLOS [28]

in the order of tens of centimeters to meters, depending on the environment. Thus, there is a need to estimate the time bias introduced by the obstacles and ultimately cancel out its effect.

1.3 Research framework

This master thesis is done under the auspices of the project *Localization in Smart Dust Sensor Networks,* in the Telecommunication Engineering Group at the University of Twente. The aim of the project is to investigate the localization issues in smart dust sensors. In this project, the methods to handle NLOS-related ranging errors are investigated, taking into account design considerations like size, complexity and power consumption. The approach taken is to gather statistics about the ranging error, exploiting certain UWB signal features. These statistics are used to identify the NLOS nodes in order to mitigate the ranging error related to NLOS situations and ultimately predict the range error in such environments. Cooperative localization schemes that are also robust to NLOS conditions are also dealt with.

In a previous masters assignment [52], range error mitigation in NLOS scenarios was addressed. This thesis addressed the issue using characteristic features. Various characteristic features (excess delay, rms delay, rise time, global peak delay, coherence bandwidth, ricean factor and path loss exponent) were extracted from the received signal. The correlation between each feature and the range error was analyzed and a relation was found between each feature and the error in ranging. Instead of using the features individually, the thesis suggests using the features jointly. Naive Bayesian regression is used to estimate the error in ranging and mitigate it accordingly. Actual measurements were used for training and testing the technique.

However, the technique used in [52] has some shortcomings. All measurements were done in the same environment with some in LOS and some in NLOS. However, all these measurements were trained and analyzed together. No effort was made to separate and accordingly treat LOS and NLOS measurements differently. Moreover, in describing a relation between characteristic features and the ranging error, a fitting curve technique was used. This fitted curve had a lot of outliers, making it less reliable. A question is also raised with regard to the regression technique used. Naive Bayesian assumes all the features to be uncorrelated. However, the features used do have some correlation. For instance between coherence bandwidth and RMS delay spread there is high degree of correlation. Assuming the features to be uncorrelated while they are actually having a high degree of correlation can make the technique less accurate. A serious note is also made in the conclusion, as the data that were used for training and testing the algorithm were the same.

One novel idea that was proposed in [52] is the use of an extrapolation technique in detecting the direct path, even under noise. However, for UWB signals which have a very small pulse width, this procedures hardly provides any improvement. From localization perspective, [52] concludes that it is better to discard NLOS measurements that to incorporate them in the overall localization. However, in the absence of enough number of anchor nodes that are in LOS, it is more effective to use the NLOS range estimate. In such cases, it is important to mitigate the NLOS range estimates before using them.

All the measurements were made in one office, and, to manifest the various environments, mobile obstacles were used (like wood, cinder, metal sheet). How that relates to the actual environments is also another question that lingers.

1.4 Research goals

The overall goal of this thesis is to overcome the shortcomings of the existing ToA ranging techniques. This thesis also aims at circumventing the shortcomings of [52] while proposing more robust methods. Measurements that are in NLOS will be treated separately from those in LOS. Moreover, in addition to the features used in [52], some additional features will be investigated. A more robust regression technique will be examined. To avoid complexity, instead of using all the features, as is the case in [52], only the most influential and promising features will be used. In our case, the issue of detecting the direct path is addressed from the perspective of SNR improvement.The ranging approach that we are going to follow is given in Figure 1.4.

The first range estimate is given by a ToA technique using first peak detection. While the first range estimate should be the final range estimate for the sensors in LOS, it is a biased one for those in OLOS/NLOS. Therefore, following the initial range estimate, channel identification is done. This identification technique is going to be based on features extracted from the received signal. This step enables us to identify if the sensor is in LOS or not. If the sensor is in OLOS/NLOS, there is a need to estimate the ranging error introduced due to blockage/reflection and ultimately cancel its effect. This process is termed as range error mitigation.

1.5 Research questions

This thesis will address the ranging problems from the ranging approach outlook given in Figure 1.4. Each block within the figure will be treated and a mechanism will be investigated to

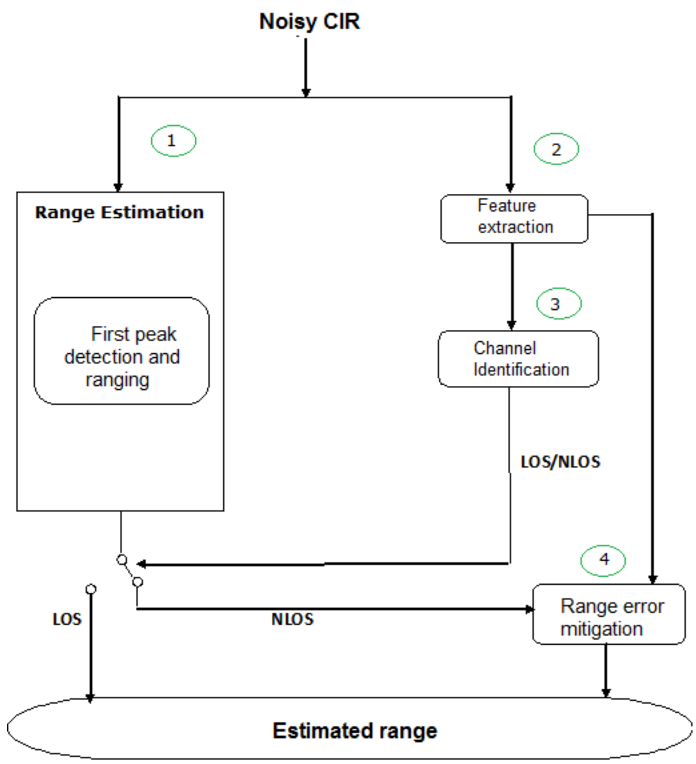

Figure 1.4: Ranging approach, flow chart

improve the outcome of each block. The questions that are addressed in this thesis are:

1. Can we improve the range estimate in low SNR situations ?

2. Can we exclusively identify sensors in LOS from those in NLOS?

3. Can the ranging errors in NLOS be estimated and mitigated?

1.6 Thesis structure

According to the research approach, this thesis is organized in as follows: Chapter 2 deals with SNR improvement using wavelet based de-noising. The motivation behind wavelet de-noising and its impact on ranging accuracy is dealt with in this chapter. Chapter 3 deals with the second research question, i.e. can we separate sensors in LOS from those in NLOS, and, if so, how? Chapter 4 looks at the third problem, mitigation. The last chapter, Chapter 5, will give an overall conclusion on the results obtained in the previous three chapters, and provide recommendations.

Chapter 2

WAVELET DE-NOISING FOR IMPROVED TIME OF ARRIVAL RANGING

In this part of the thesis, details of the ToA technique are discussed. One of the main steps in ToA ranging is the first peak detection. The first peak defines the initial distance estimate.

Under a noisy environment, the first peak could be covered by the noise, making it undetectable. In such cases, it is important to improve the SNR, and, by doing so, improve the detectability of the first peak. In this regard, we will investigate a means to improve the SNR and ultimately improve the detectability of the direct path. A wavelet based de-noising technique is employed for improving the SNR. All analysis and testing is subject to actual realistic measurements.

According to the flow chart in Figure 2.1, the block within the highlighted box is treated in this chapter. Initially, the fundamentals of ToA ranging are discussed. Following, a brief discussion on various first peak detection algorithms is treated. In order to asses the importance of de-noising in ranging, in Section 2.3 the basics of wavelets and wavelet de-noising techniques are presented. Evaluation of the de-noising technique with actual measurements is presented in

Section 2.4. The conclusion of this chapter is made in Section 2.5.

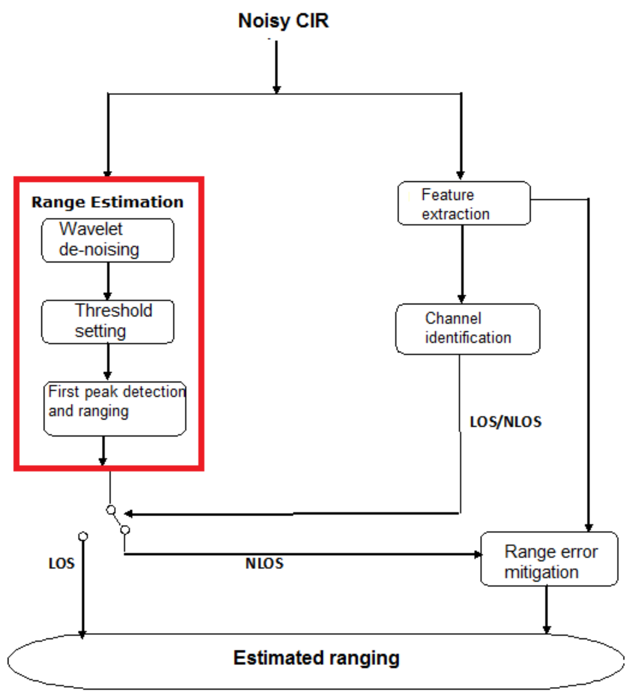

Figure 2.1: Ranging approach, flow chart

2.1 Fundamentals of time of arrival ranging

As mentioned in the previous chapter, ToA ranging is based on measuring the propagation time, i.e. the amount of time a signal takes to travel from a transmitter to a receiver. This time measurement is translated to distance by using the velocity of the signal in the medium.

One of the challenges in ToA is detecting the peak corresponding to the direct path. Figure 2.2 shows examples of actually received UWB signals. Received signals in the case of LOS and

NLOS are presented. Note that the estimated channel impulse response can be obtained from the received signal by correlating it with the known transmitted signal. Therefore, throughout the thesis "received UWB signal" is used to mean estimated channel impulse response.

To find the time of flight, we first need to locate where the first peak is. The first peak will signal the first point in time where the transmitted signal reaches the receiver. Geometrically, this represents the shortest path between the two nodes. The rest of the impulse response consists of delayed versions of the transmitted signal, also known as multipaths.

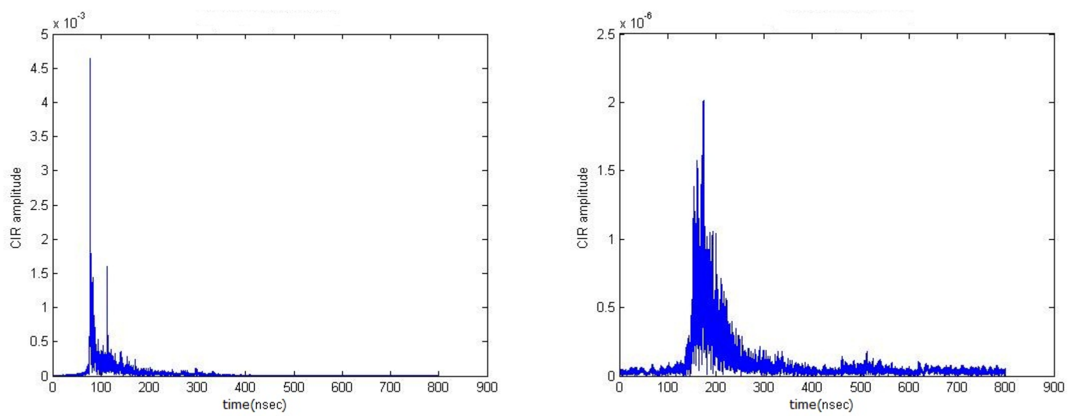

(a) (b)

Figure 2.2: Measured UWB signals in the case of LOS (a) and NLOS (b)

In order to find the first peak, it is important to determine the detection threshold. The first peak is chosen as the first of those peaks that are greater than the detection threshold. Underestimating the noise could result in lower detection level resulting in a false detection, i.e. if the threshold is set too low, peaks due to noise could be wrongly considered as the first peak. This is illustrated in Figure 2.3a. A False alarm would result in estimating the distance to be shorter than it actually is.

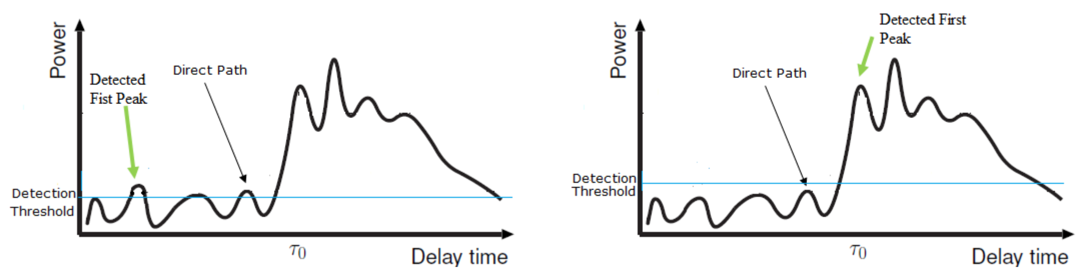

(a) False Alarm of direct path

(b) Missed detection of direct path

Figure 2.3: Possible errors in detecting the direct path

Another situation could be over-estimating the noise, and, accordingly, setting the detection threshold higher than what it should be. In such cases the first peak is missed, causing a positive bias in the distance estimated; see Figure 2.3b. This phenomena is termed as missed detection.

Therefore, there is a need to calibrate the detection threshold with good accuracy. Various techniques have already been proposed, as will be explained in Section 2.2.

A situation that is more interesting occurs when the first peak is buried under noise. In such cases, no matter how the detection threshold is set, you will never be able to detect the first peak. Thus, in such specific environments, it becomes imperative to improve the signal power with respect to the noise. In other words, a technique has to be employed to improve the detectability of the first peak. Details of possible techniques are presented in Section 2.3.

2.2 Thresholding techniques in time of arrival ranging

Various thresholding techniques have already been proposed in literature [25, 37, **?**]. A typical method is to choose the threshold a few dBs above the noise level. Noise level estimation can be done from the first few samples of the received waveform. A similar but still distinct approach is to set the threshold based on the global peak, i.e. the threshold is a few dBs below the global peak [25].

Still, another proposed method is the *delay dependency (DD)* based threshold selection [38]. This technique utilizes the dependency of the signal strength on distance. As we increase the distance, the strength of the received signal will decrease. In this system, the parameters for defining the threshold need to be optimized and customized to the given application and as such can not be generalized.

Both global peak based thresholding and the noise level based thresholding have comparable degree of complexity while their accuracy is the same. Thus, any one of the two can be used. In our case, we are going to use the noise level based thresholding.

A further extension to those techniques would be to use an extrapolation technique to find the starting of the first peak. This has been proposed in [50] for narrowband signals and in [52] for UWB signals. Large pulse width (small bandwidth) signals benefit from this techniques because of the long leading edge present. However, UWB signals have a narrow pulse width, limiting the effectiveness of the algorithm. Thus, this technique might be effective for narrowband signals but not for UWB signals.

2.3 Improving the SNR

2.3.1 Motivation

As mentioned above, how precisely we identify the direct path is a critical issue in the overall ranging performance. This holds in both low and high SNR conditions. In this section, we will look at how we can improve the SNR of a given situation by making use of a wavelet technique. This becomes imperative in case of low SNR environments where the direct path could be buried under noise.

There are different ways of improving the SNR. Often, increasing the power of the information signal at the transmitter side could easily improve the SNR. However, for UWB signals this might not be possible as there is a limit on the maximum transmission power.

Another approach is to increase the SNR at the receiver side. In doing so, a matched filter (MF) is commonly used. A matched filter correlates the received signal with a template of the transmitted signal.

A similar technique but with different approach is the so called de-noising. The most common type of de-noising technique is wavelet de-noising (WD). Wavelets utilize the unique behavior of noise to separate the noise from the information signal. The motivation for wavelet de-noising comes from the inherent behavior of indoor environments. Indoor environments are made of a number of reflectors and obstructions, which ultimately result in multipaths. How those multipaths add up to provide the received signal is something that cannot be predicted. As such, finding the exact template of the transmitted signal at the receiver may not be the most effective method to use. Wavelets try to circumvent this by using scaling and translation techniques. A more detailed analysis of wavelets can be obtained in [42]−[46].

2.3.2 Basics of wavelet de-noising

To analyze signals in both time and frequency domain, special types of Fourier transform like Short Time Fourier transform (STFT) can be used. However, in STFT, the time and frequency resolutions are in a trade-off. Using wavelets, it is possible to have variable time and frequency resolutions. This enables us, for instance, to obtain a detailed frequency analysis by increasing the time resolution, while to look at, say, discontinuities or peaks, we can have shorter time resolutions.

Basically, we have two types of wavelet transforms. The *Continuous Wavelet Transform* (CWT) is mathematically defined as

$$\gamma(s,\tau) = \int_{\infty}^{\infty} f(t)\,\psi^*_{(s,\tau)}(t)\,\mathrm{d}t, \tag{2.3.1}$$

where * denotes complex conjugation. The function $f(t)$ is decomposed into a set of basis functions, called the wavelets. The variables s and τ are termed as scale and translation.

The wavelets $\psi_{(s,\tau)}(.)$ are generated from the so called *Mother Wavelet* $\psi(.)$ as

$$\psi_{(s,\tau)}(t) = \frac{1}{\sqrt{s}}\psi\left(\frac{t-\tau}{s}\right) \tag{2.3.2}$$

The factor $s^{-1/2}$ is for energy normalization across the different scales.

The function $f(t)$ can be re-constructed from its wavelet transform $\gamma_{(s,\tau)}$ using the formula

$$f(t) = \int_{0}^{+\infty}\int_{-\infty}^{+\infty} \frac{1}{s^2\sqrt{s}}\gamma_{(s,\tau)}\tilde{\psi}\left(\frac{t-\tau}{s}\right)\mathrm{d}\tau.\mathrm{d}s, \tag{2.3.3}$$

where $\tilde{\psi}$ is a dual function of ψ and it should satisfy,

$$\int_{0}^{+\infty}\int_{-\infty}^{+\infty} \frac{1}{s^3}\psi^*\left(\frac{t_1-\tau}{s}\right)\tilde{\psi}\left(\frac{t-\tau}{s}\right)\mathrm{d}\tau.\mathrm{d}s = \delta(t-t_1) \tag{2.3.4}$$

The Discrete Wavelet Transform (DWT) is a special case of the wavelet transform that provides a compact representation of a signal in time and frequency that can be computed efficiently. Mathematically this is given by,

$$\psi_{(j,k)} = \left(s_o^j\right)^{-1/2}\psi\left(\frac{t-k\tau_o s_o^j}{s_o^j}\right) \tag{2.3.5}$$

j and k are integers, $s_o > 1$ is a fixed dilation step and τ_o is the translation step.

In wavelets, unlike in Fourier transforms, the *mother wavelet* is not uniquely specified. Normally, there are different types of mother wavelets (Haar, Daubechies, Coiflets, Symelts, and Biorthognal), their basic difference being in how they define the wavelet and the scaling signal.

For a single pulse transmitted, the received UWB signal under multipath can be modeled as,

$$r(t) = \sum_{l=0}^{L} \alpha_l \omega(t - t_l) + n(t) \tag{2.3.6}$$

where $\omega(t)$ is the transmitted pulse template of duration T_{p}, α_l and t_l are the amplitude and time delay of the l-th multipath, L presents the number of propagation paths, and $n(t)$ is the additive white Gaussian noise (AWGN). This can be written in vector form as

$$\mathbf{r} = \mathbf{s} + \mathbf{n}, \tag{2.3.7}$$

where the elements of **s** represents samples of the signal part and the elements of **n** the samples of the noise part of the received signal. In removing the noise using wavelets, there are three steps proposed in [42]:

1. Calculate the discrete wavelet transform (DWT) of the signal
2. Threshold the wavelet coefficients
3. Compute the inverse DWT

The first step in wavelet de-noising is performed by multiplying the received waveform **r** with a $M \times M$ orthonormal wavelet matrix **W**, as

$$\mathbf{r}_w = \mathbf{W}\mathbf{r} = \mathbf{s}_w + \mathbf{n}_w \tag{2.3.8}$$

with

$$\mathbf{s}_w = \mathbf{W}\mathbf{s} \tag{2.3.9}$$

$$\mathbf{n}_w = \mathbf{W}\mathbf{n} \tag{2.3.10}$$

and

$$\mathbf{W} = \left\{ \begin{array}{cccccc} w_1(0) & w_1(t_s) & w_1(2t_s) & \cdots & \cdots & w_1((M-1)\,t_s) \\ w_2(0) & w_2(t_s-\tau_1) & w_2(2t_s-\tau_1) & \cdots & \cdots & w_2((M-1)\,t_s-\tau_1) \\ w_3(0) & w_3(t_s-\tau_2) & w_3(2t_s-\tau_2) & \cdots & \cdots & w_3((M-1)\,t_s-\tau_3) \\ \vdots & \vdots & \vdots & \vdots & \vdots & \vdots \\ \vdots & \vdots & \vdots & \vdots & \vdots & \vdots \\ w_M(0) & w_M\left(t_s-\tau_{(M-1)}\right) & w_M\left(2t_s-\tau_{(M-1)}\right) & \cdots & \cdots & w_M\left((M-1)\,t_s-\tau_{(M-1)}\right) \end{array} \right\} \tag{2.3.11}$$

represents $M \times M$ matrix representing the delayed and sampled version of $w(t)$.

The elements of $\mathbf{r}_w$ are the wavelet coefficients.

The second step in wavelet de-noising is finding out which of those coefficients are due to noise and which are due to the signal. Noise has the specific character of being wideband and having higher frequency. Because of this, the noise coefficients are usually small compared to the coefficients due to the signal [42, 43]. Determining which of the coefficients are due to noise and which are not is termed as wavelet thresholding.

There are two common methods of wavelet thresholding [42, 43]: *Hard* and *Soft* threshold selection. We also the *hyperbolic shrinkage* thresholding methods. However, both soft thresholding and hyperbolic thresholding have a smoothing effect, i.e. apart from discarding the low coefficients, they also reduce the magnitude of the coefficients that are retained. These techniques are mostly used in image processing. In our case, we would like to detect the peaks. Thus, smoothing them is something we do not want to do. Therefore, hard thresholding is preferred.

To set the threshold, multiply the above $\mathbf{r}_w$ with a diagonal matrix

$$\mathbf{H} = \mathrm{diag}[h(1), h(2), h(3), ...h(M)]$$

where diag() represents a matrix whose diagonal is made of the elements $h(1), h(2), h(3), ...h(M)$ while the rest of the elements of the matrix are zero.

The inner values of $\mathbf{H}$ are selected by the hard threshold method, i.e.

$$h_{\mathrm{hard}}(i) = \begin{cases} 1, & |\mathbf{r}_w(i)| > \delta \\ 0, & |\mathbf{r}_w(i)| \le \delta \end{cases} \tag{2.3.12}$$

where δ is the threshold from [42, 43] given by

$$\delta = \sigma\sqrt{2\times\log_{10}(M)}$$

The variance σ^2 of the noise can be estimated from the first few noise samples as

$$\hat{\sigma}^2 = \frac{1}{N-1}\sum_{i=1}^{N}\left(r(t_i) - \hat{\mu}\right)^2, \tag{2.3.13}$$

where $\hat{\mu}$ is the estimated sample mean and N the number of samples used to estimate the noise variance.

The last step in the de-noising process would be to reconstruct the signal by taking the inverse wavelet transform, i.e.

$$\hat{\mathbf{r}} = \mathbf{W}^T\tilde{\mathbf{r}}_{\mathbf{w}} = \mathbf{W}^T\mathbf{H}\mathbf{W}\mathbf{r} \tag{2.3.14}$$

which is the inverse DWT operation to the de-noised wavelet coefficients $\widetilde{\mathbf{r_w}} = \mathbf{Hr}$, where $\hat{\mathbf{r}}$ represents the resulting estimate of $\mathbf{s}$.

Moreover, it is also possible to recursively decompose the signal to get finer detail and more general approximation [47]. This is called multi resolution analysis (MRA). This is made so as to analyze the signal at different time and frequency resolutions. It is designed to give good time resolution and poor frequency resolution at high frequencies and good frequency resolution and poor time resolution at low frequencies.

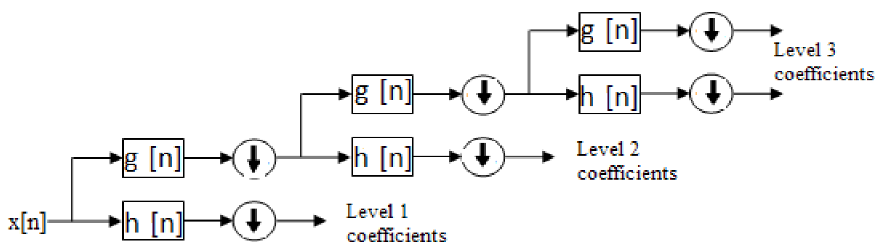

Figure 2.4: Multi-resolution analysis using filter banks h[n] is a high pass filter and g[n] is a low pass filter

At each decomposition step, the low frequency components are analyzed with a higher degree of resolution. The number of steps performed is termed the decomposition level.

The performance of wavelet de-noising depends on the type of wavelet function, thresholding technique, and decomposition level applied.

2.3.3 Wavelet selection and level of decomposition

There are two ways in which we can select the mother wavelet: based on visual inspection of the signal, i.e. looking at what the signal looks like and relating it to one of the mother wavelets, or based on correlation between the mother wavelet and the de-noised signal. In our case, we use the correlation method as that is going to give us analytical results to base our decision.

To do so, the channel model CM3 (indoor office, LOS) from IEEE 802.15.4a is used. As is shown in Figure 2.5, sample impulse responses are generated using the 802.15.4a channel model. Noise (AWGN) is added to those impulse responses. These noisy impulse responses are then de-noised using wavelets. To see the effectiveness of the de-noising, the correlation coefficient between the original signal and de-noised signal is calculated. This procedure is done for different types of wavelet functions.

SNR is defined as

$$\mathrm{SNR} = 10\log_{10}\left(\frac{P_\mathrm{s}}{P_\mathrm{n}}\right), \tag{2.3.15}$$

where P_s is the signal power and P_n is the noise power.

The correlation coefficient is given by

$$c_{x,y}\left(j\right) = \frac{\sum_{i=1}^{n}\left(x_i - \overline{x}\right)\left(y_i - \overline{y}\right)}{\sqrt{\sum_{i=1}^{n}\left(x_i - \overline{x}\right)^2\left(y_i - \overline{y}\right)^2}} \tag{2.3.16}$$

where $\overline{x}$ and $\overline{y}$ are the sample means of x and y, i represents the sample index while j represents the realization index. x and y represent the original and the de-noised signals. This is done for the 1000 realizations. To obtain the mean correlation coefficient,

$$\overline{c} = \sum_{j=1}^{n} c_{x,y}\left(j\right) \tag{2.3.17}$$

$c_{x,y}\left(j\right)$ is the correlation coeifficent corresponding to the given realization.

For each wavelet type, 1,000 realizations are generated, and for each case a correlation value is obtained. For comparison purposes, the mean of these correlation values is taken. High correlation would mean that the de-noised signal resembles more precisely to the impulse response generated.

Being the most common type of wavelets used in de-noising, Daubechies6, symlet4, symlet8 and coiflet2 wavelets are investigated.

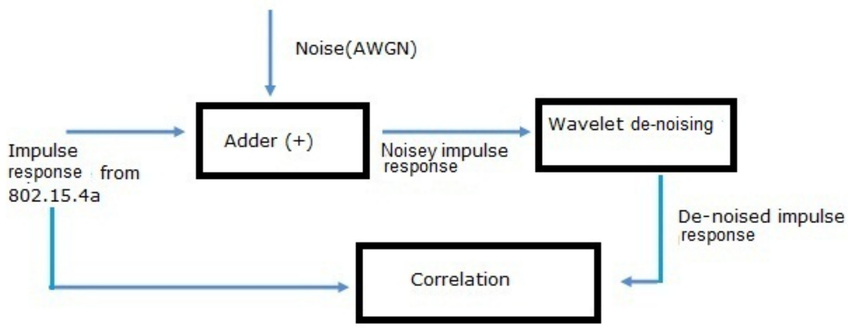

Figure 2.5: Wavelet selection based on correlation

Tabulated in Table 2.1 is the mean correlation value for different SNRs. For all tested wavelets, the mean correlation value increased as the SNR increased. For a given SNR, the mean correlation values for the various wavelets are similar with a difference only after the second digit. This implies that, at a given SNR, the performance of the various wavelets is comparable.

Looking at the shapes of the various wavelet signals (see Figure 2.6), all the wavelet signals, except Daubechies are symmetric around the maximum peak. It is mentioned in [40, 51], Daubechies 6 , because of its asymmetry would be more appropriate to capture the the first peak in LOS situations. This was not confirmed in our analysis. However, since we have concluded that all have comparable performance, taking the suggestion of [40, 51], we have opted to use db6.

Table 2.1: Mean correlation between de-noised and original signal for various wavelet types

SNR	Daubechies6 (db6)	Symlet4 (sym04)	Symlet8 (sym08)	Coiflets2 (coif 02)
0	0.7836	0.7879	0.7852	0.7861
5	0.8456	0.8497	0.8488	0.8495
10	0.9031	0.9069	0.9061	0.9063
15	0.9461	0.9477	0.9473	0.9479
20	0.9715	0.9729	0.9722	0.9724

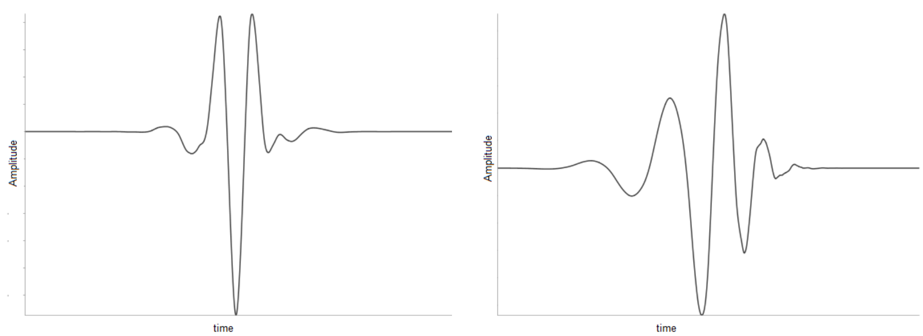

(a) Symlet 8 wavelet (b) Daubechies 6 wavelet

Figure 2.6: Symlet 8 and Daubechies 6 wavelets

As mentioned before, the optimal degree of decomposition depends on the level of the SNR. Decomposition also incorporates computational complexity in the system. In our case, a decomposition level of 4 is chosen which has moderate complexity.

The computational complexity (multiplication operations) incurred by db6 based wavelet de-noising is $o(M)$, M being the number of samples of the received waveform [40]. For a decomposition level of N, the complexity is given by $o(N \cdot M)$.

2.3.4 SNR improvement using wavelets

From Section 2.3.2, we have concluded that hard thresholding is the most suitable wavelet tresholding. In order to investigate the effectiveness of wavelet de-noising at different SNRs, a test bench was developed as shown in Figure 2.7. 1,000 realizations of the channel impulse response were generated using the 802.15.4a channel model, CM3 (indoor offices LOS). From all the channel models, CM3 is used, since the actual measurements (explained in the coming section) used to test the performance of wavelet de-noising are made in an indoor office.

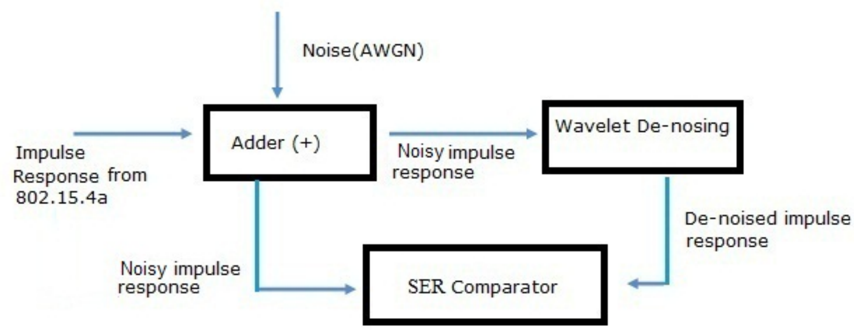

Figure 2.7: Wavelet threshold selection method

AWGN was added to each realization. Following is a wavelet de-noising block, where de-noising is done using db6 and hard thresholding. As a figure of merit, a comparison is made between the error before and after de-noising i.e. mean signal to error gain is used as a criterion. Mathematically,

$$\triangle \mathrm{SER[dB]} = \mathrm{SER_{out}[dB]} - \mathrm{SER_{in}[dB]} \tag{2.3.18}$$

$$\mathrm{SER_{in}[dB]} = 20\log\left(\frac{||\mathbf{s}||}{||\mathbf{n}||}\right) \tag{2.3.19}$$

$$\mathrm{SER_{out}}[\mathrm{dB}] = 20\log\left(\frac{||\mathbf{s}||}{||\mathbf{s}-\hat{\mathbf{s}}||}\right) \tag{2.3.20}$$

where the elements of **s** are the signal samples, **n** the noise samples, $\hat{\mathbf{s}}$ is the samples of the de-noised signal, $\mathrm{SER_{in}}$ corresponds to the input signal to error ratio[1] and $\mathrm{SER_{out}}$ corresponds to the output signal to error ratio. $||.||$ represents Euclidean norm.

As can be inferred from Figure 2.8, we can see that, as the signal to noise ratio increases, the improvement made by the wavelet de-noising technique decreases. In fact, at higher SNRs (10 dB or more), it can be observed that, the technique employed could have a negative effect. This is because at high SNRs, there is not much noise to remove, and, thus, wavelets remove some of the information signal, causing a decrease in SNR.

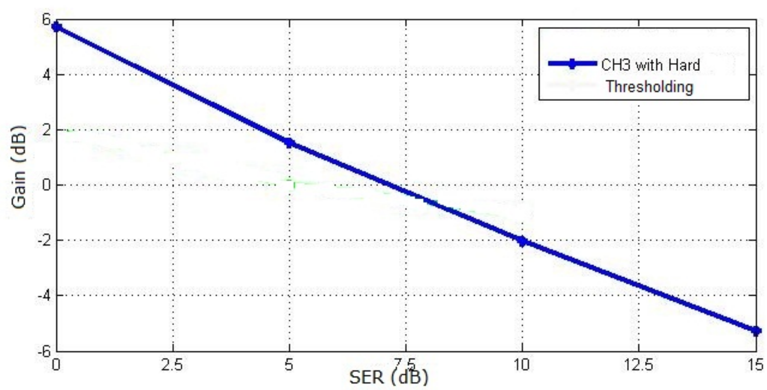

Figure 2.8: SER improvement using hard thresholding

[1] $\mathrm{SER_{in}}$ is equivalent to $\mathrm{SNR_{in}}$ but that does not hold for $\mathrm{SER_{out}}$ because after de-noising, it is possible that the information signal has also been affected.

2.4 Impact on ranging performance

So far, we have investigated the importance of wavelet de-noising and how it can be used to improve the SNR in a given environment. Our analysis has been based on the 802.15.4a channel model. Nevertheless, the ultimate goal is to improve the detectability of the first peak and accordingly decrease the range error. This objective cannot be examined using the 802.15.4a channel model as the channel model lacks the actual distance information. Moreover, to make the results more conclusive it is important that the test is made with actual measurements. Therefore, this section addresses the impact of wavelet de-noising on the detectability of the first peak and the range error using actual measurements.

2.4.1 NIST campus measurements

Measurements made in the National Institute of Standards and Technology (NIST) in [28] are used in our analysis. The measurements were conducted in four different rooms, constructed from different materials (dominantly), in the NIST campus in Gaitherburg, Maryland, USA. The measurements cover a distance up to 45 m, while the number of walls present in between varies greatly. Overall, 200 measurements were performed, 50 in each room. The four rooms are NIST North (sheet rocks/aluminum studs), Child Care (plaster/wooden studs), Sound (cinder blocks) and Plant (steel). Out of 50 measurements, in each room 40 are either in OLOS or NLOS, while 10 are in LOS.

As the measurements are made in actual environments they are suitable for our analysis. Moreover, the measurements were made in different office environments that are dominantly made of different materials, and, since they cover large distances, they are found to be appropriate for our case. The measurements include all possible scenarios (LOS and NLOS).

2.4.2 Wavelet de-noising

Looking at Figure 2.9, the samples before the first peak (direct path) are noise samples, while, the last few samples, starting from N_2 are also noise samples. The part of the received waveform containing the signal information is located between $N_1 - N_2$.

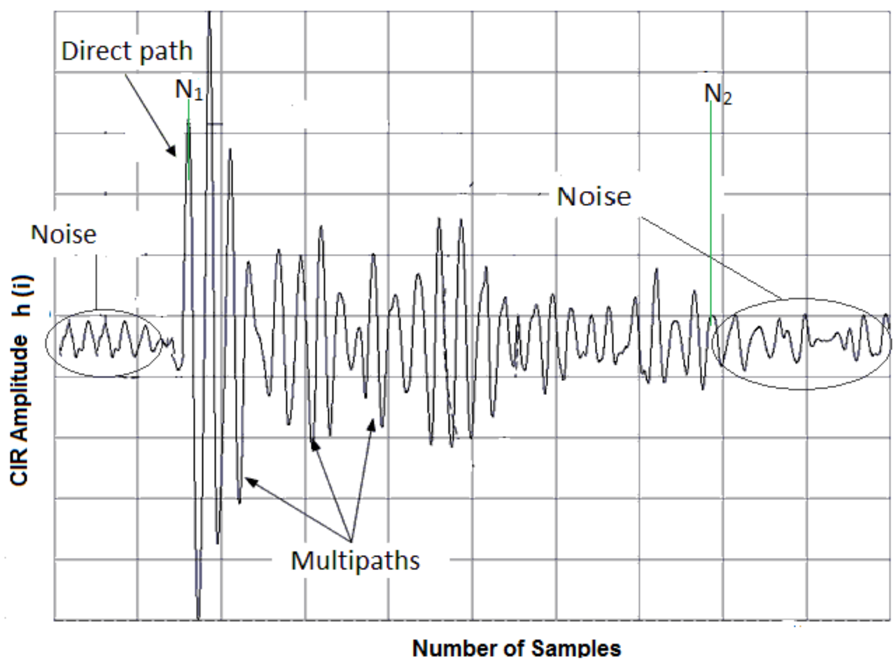

Figure 2.9: Sample impulse response

Accordingly, the noise power per sample can be estimated as

$$\hat{P}_n = \frac{\sum_{i=0}^{(N_1-1)} h^2(i)}{N_1} \tag{2.4.1}$$

and the estimated signal power per sample is

$$\hat{P}_{\mathrm{s}} = \frac{\sum_{i=N_1}^{(N_2-1)} \left(h^2(i) - \hat{P}_{\mathrm{n}}\right)}{N_2 - \mathrm{N}_{\mathbf{1}}} \tag{2.4.2}$$

Then, the estimated SNR is

$$\mathrm{SNR} = 10 \log_{10} \left(\frac{\hat{P}_{\mathrm{s}}}{\hat{P}_{\mathrm{n}}} \right) \tag{2.4.3}$$

As we have the knowledge of the actual distance, the first peak (N_1) is determined from that information. Using the samples before the first peak, the noise energy per sample is estimated.

To determine N_2, we need to find the sample after which only noise samples are present. To do so, we have used a windowing method. A window with N_1 sample is used. This window is moved across the the received waveform starting from N_1 . At each step, the mean energy within the window is measured. The moment the mean energy of in the window is equal to or less than the mean noise energy (calculated earlier), then, samples in that window and the samples after that are considered to be made of noise. Thus, the beginning of that window is taken as N_2.

Out technique need to be tested at both low and high SNRs. As such, each measurement is manipulated i.e. a Gaussian random variable is added to each sample with a variance such that the total variance meets the required noise level. In such a manner, SNR values of −12 dB, −9 dB, −6 dB, −3 dB, 0 dB, 3 dB, 6 dB, 9 dB and 12 dB are investigated.

In order to determine the range error at different SNRs, first, the detection threshold needs to be set. While, how to set the detection threshold is another question, in our case, we have decided to set or define the detection margin and ultimately the detection threshold.

The detection threshold (P_{T}) chosen as,

$$P_{\mathrm{T}}\,[\mathrm{dB}] = \hat{P}_n\,[\mathrm{dB}] + \triangle P\,[\mathrm{dB}] \tag{2.4.4}$$

where $\triangle P$ represents the detection margin.

In doing so, for a given SNR, the following steps are taken,

1. First LOS and NLOS measurements are separated

2. For all LOS measurements, an initial detection margin (0) is set, and, accordingly, the range error for each LOS measurement is determined.

3. The detection margin is increased by 0.1 and the range error is determined for each LOS measurements again.

4. Step 3 is repeated until the maximum possible detection margin is set. The maximum detection margin is a detection margin where all measurements lay below the detection threshold.

5. The mean square error criterion is used in opting for the optimal detection margin.

The mean square error (MSE) is given by

$$\text{MSE} = \frac{1}{N}\sum_{i=1}^{N}\left(\varepsilon_{\mathrm{r}}\left(i\right)\right)^{2} \tag{2.4.5}$$

where N is the number of LOS or NLOS measurements and $\varepsilon_{\mathrm{r}}(i)$ is the range error associated with a given measurement $\hat{i}$.

Steps 2−5 are also done for the NLOS measurements.

Now that the detection margin for each SNR value has been specified, we can estimate the range and accordingly the range error. Below are some of the results that represent the overall performance of de-noising.

Figure 2.10 shows a comparison between the range errors before and after de-noising. This comparison is made for the LOS measurements. The regions I and III represent Regions where the range error has increased after de-noising, while Regions II and IV show regions where the range error has decreased.

The NIST measurements are made with a receiving window of 800 ns. Multipaths within the 800 ns range or equivalently around 240 m can be detected. In Figure 2.10, the points with a range error of greater than 150 m are outliers. They are measurements where the receiver does not detect an information signal. This is because, in those cases, the signal is below the detection threshold. For analysis purposes, their range estimate is marked as 240 m i.e. the maximum possible range estimate of the receiver. Their range error is calculated by subtracting the actual distance from the range estimate (240 m).

When the SNR is −12 dB, only 32.5% of the LOS measurements were detected, while after de-noising the signals, around 65% of the measurements were detected. Similarly, for −9 dB, only 45% of the LOS measurements were detected, while 80% of the measurements were detected after de-noisng. Similar results also hold during the NLOS situations.

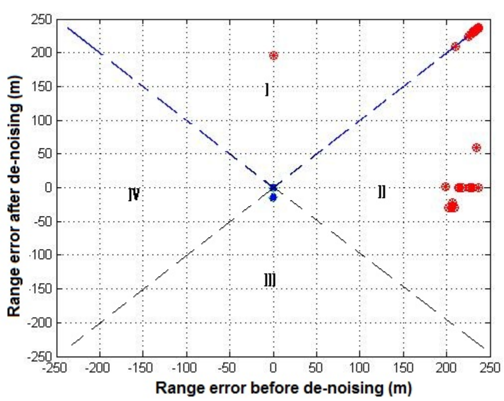

(a) SNR = −12 dB

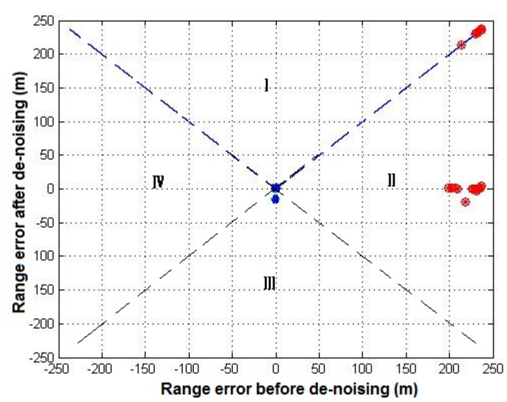

(b) SNR = −9 dB

Figure 2.10: Range error comparison for LOS measurements at SNR = −12 dB and −9 dB

However, as can be inferred from the figures, at SNR = −12 dB, one measurement that was detected before de-noising was undetected after de-noising. This is mainly because of the error in setting the detection threshold. As the detection threshold is set based on the detection margin that is optimal from the overall measurements perspective, it is possible in some cases that an overestimate of the thresholding can take place. Nevertheless, in LOS, the overall detectability performance has improved for those SNRs that are below 6 dB, as is given in Table 2.2a. For NLOS measurements, the detectability improvement holds for all SNR values.

Around the (0,0) coordinates, what we see in Figure 2.11, is that those measurements that result in a low range error before de-noising, result in an increased range error after de-noising. Thus, there is a degradation in the accuracy of those measurements that were already within small range error before de-noising.

Table 2.2: Detectability comparison before and after de-noising

(a) LOS

SNR	Signal detectability (%)	
	Before de-noising	After de-noising
−12 dB	32.5%	65%
−9 dB	45%	80%
−6 dB	62.5%	92.5%
−3 dB	52.5%	75%
0 dB	87.5%	92.5%
3 dB	97.5%	100%
6 dB	100%	100%
9 dB	100%	100%
12 dB	100%	100%

(b) NLOS

SNR	Signal detectability (%)	
	Before de-noising	After de-noising
−12 dB	24.4%	60%
−9 dB	27.5%	55%
−6 dB	35.6%	71.2%
−3 dB	38.1%	73.7%
0 dB	55.6%	84.4%
3 dB	76.8%	89.4%
6 dB	83.7%	91.25%
9 dB	95%	97.5%
12 dB	96.25%	100%

Looking at the NLOS cases, Figure 2.12 gives the zoomed in plot for SNR = −12 dB and −9 dB. From the figure we can see that, for the majority of the measurements, the range error has decreased after de-noising. In both cases a large share of the measurement is within Region II showing an improvement in the range error.

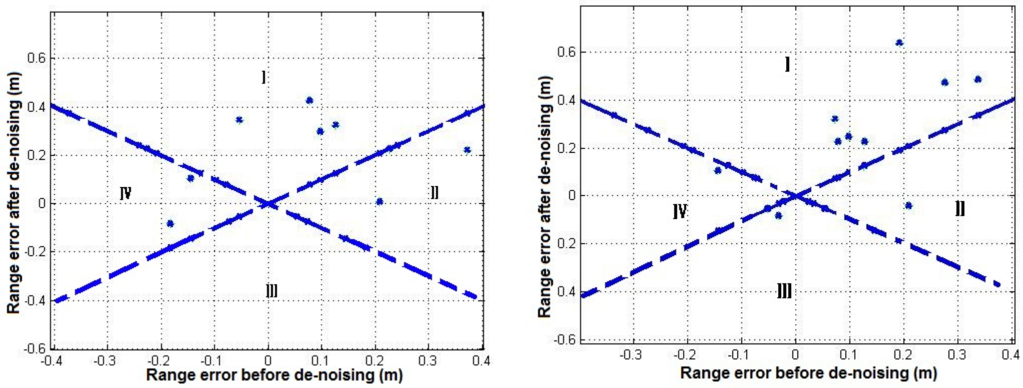

(a) SNR = −12 dB (b) SNR = −9 dB

Figure 2.11: Range error comparison for LOS measurements (zoomed) at SNR = −12 dB and −9 dB

In order to show the overall impact of wavelet de-noising on ranging, CDF plots are used. Figure 2.13 presents the CDF plots for LOS measurements at SNR= −12 dB, −9 dB, 9 dB and 12 dB. The figures are zoomed in to concentrate on the important part of the graph, i.e. the small range errors.

The results show that as the SNR increases, the number of measurements that are within 1m range error increases. This is intuitive because, as SNR increases, the detectability of the first peak also increases. Comparing the results before and after de-noising, for low SNR values there is an improvement in the number of measurements that are within 1m in range error. However, for high SNR values like 9 dB and 12 dB, the number decreased after de-noising. This is attributed to what is discussed in Section 2.3.4, where at high SNRs, wavelet de-noising will affect the information signal part of the received waveform, as there are not much of a noise to remove. This results in assuming some peaks that are due to information signal as noise and thus, removing them.

So far, it has been shown that wavelet based de-noising increased the number of measurements

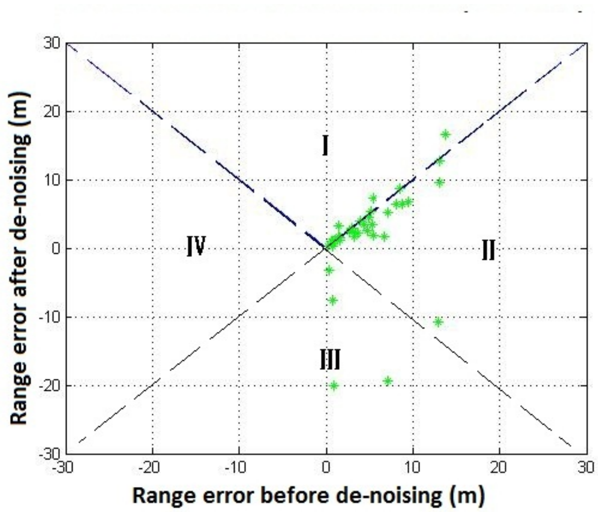

(a) SNR =−12 dB

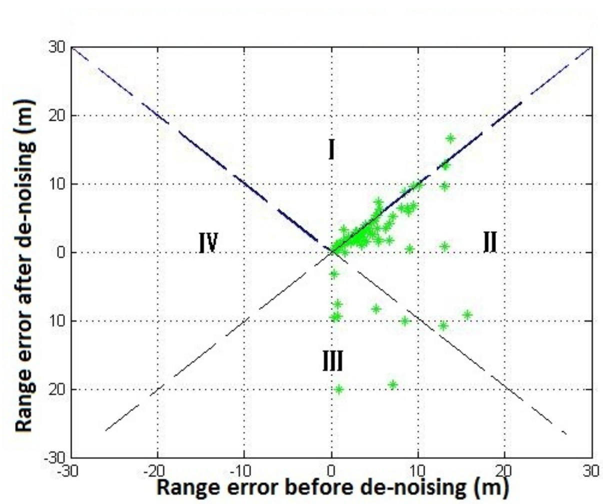

(b) SNR =−9 dB

Figure 2.12: Range error comparison (zoomed in) for NLOS measurements at SNR = −12 dB and −9 dB

that are detectable. Moreover, de-noising has also improved the number of measurements that are within 1 m in range error. However, in some cases, de-noising has also increased the range error in those measurements that had low range error before de-noising. While those analysis give us an insight about the effect of wavelet de-noising, the ultimate criterion should be on whether de-noising has increased the number of measurements that are usable for localization.

As the the expected accuracy with UWB localization is in cm level, we are going to assume any measurement that is within 1 m in range error is usable. This is true for LOS measurements. However, for NLOS measurements, there is a error mitigation process before they are actually used for localization. Mitigation processes is where the range error is estimated and ultimately deducted from the range estimate (This is treated in Chapter 4). As such, for NLOS measurements the usable range error can be taken roughly up to 10 m.

Therefore, Table 2.3a, gives the usable number of LOS measurements before and after de-noising, while similar results for NLOS measurements are given in Table 2.3b.

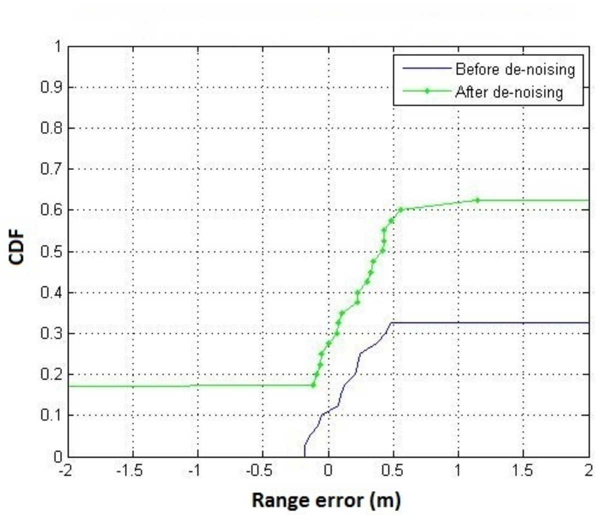

(a) SNR = −12 dB

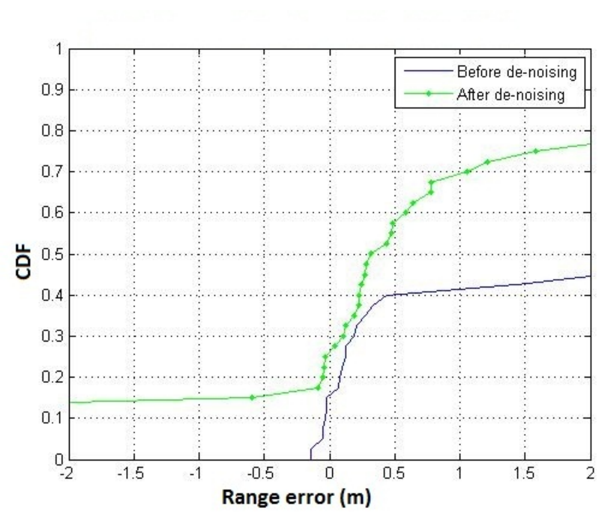

(b) SNR = −9 dB

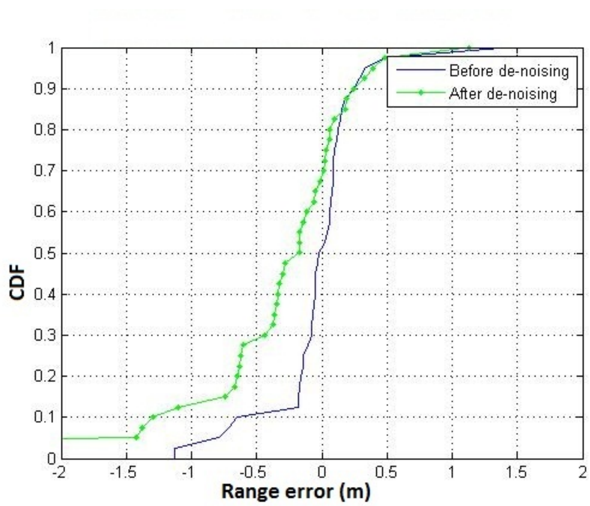

(c) SNR = 9 dB

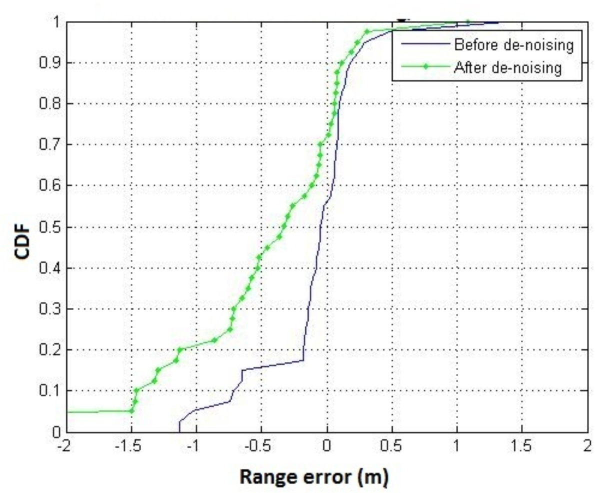

(d) SNR = 12 dB

Figure 2.13: CDF of range error for LOS measurements at SNR =−12 dB, −9 dB, 9 dB and 12 dB

Table 2.3: Usable number of measurements in both LOS and NLOS cases

(a) Usable number of LOS measurements

SNR	Usable measurements (%)	
	Before de-noising	After de-noising
−12 dB	32.5%	45%
−9 dB	40%	55%
−6 dB	57.5%	72.5%
−3 dB	50%	70%
0 dB	82.5%	85%
3 dB	85%	82.5%
6 dB	95%	90%
9 dB	95%	85%
12 dB	92.5	77.5%

(b) Usable number of NLOS measurements

SNR	Usable measurements (%)	
	Before de-noising	After de-noising
−12 dB	21.25%	44.37%
−9 dB	25%	43.75%
−6 dB	30%	56.87%
−3 dB	33.75%	61.25%
0 dB	43.75%	68.75%
3 dB	66.87%	79.37%
6 dB	76.88%	77.5%
9 dB	91.25%	83.15%
12 dB	92.5	88.75%

For LOS cases, the number of measurements within the usable range has increased by an average of 15−20%, in low SNR situations. However, at high SNRs, i.e, SNR values greater than 3 dB, there is a decrease in the number of usable measurements. This has to do with the adverse effect of wavelet denoising, mentioned in Section 2.3.4.

For NLOS measurements, for low SNR values, the number of usable measurements on average has increased by 20−35%. However, for the same reasons mentioned before, at high SNR values, de-noising has decreased the number of usable measurements.

An overall evaluation of the performance of wavelet de-noising can be done with the help of the root mean square error (RMSE). Mathematically, the RMSE is given by the square root of 2.4.5, i.e.

$$\mathrm{RMSE} = \sqrt{\frac{1}{N}\sum_{i=1}^{N}(\varepsilon_r(i))^2} \tag{2.4.6}$$

where N represents the total number of measurements and ε_r is the range error.

Figure 2.14 gives the RMSE for the usable measurements in LOS and NLOS measurements. In the LOS cases, the RMSE is increased after de-noising, with a maximum increase of 40 cm in the case of SNR= −6 dB. Knowing that we have a 20% increase in the number of usable measurements at SNR= −6 dB, the increase in RMSE, can be attributed to the increased number of usable measurements. Similarly, for NLOS, in most cases, the RMSE is higher after de-noising.

At high SNRs, the increase in RMSE is due to the negative effect that de-noising has at high SNRs.

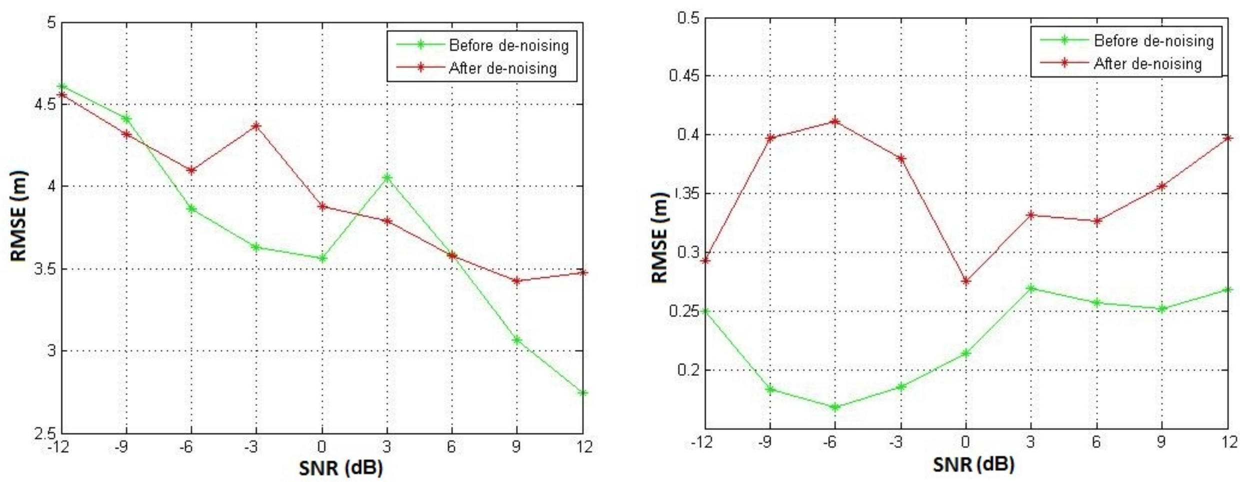

(a) NLOS (b) LOS

Figure 2.14: RMSE for LOS and NLOS measurements at different SNR values

2.5 Conclusion

In this chapter, we have looked at ways to improve the detectability of the signal, and, most importantly, the detectability of the first peak using wavelet de-noising. Wavelet de-noising has improved the detectability of those signals that are buried under the noise. This was true for both LOS and NLOS cases. By using wavelets, we are able to improve the SNR and ultimately improve the detectability of the first peak that corresponds to the direct path. Under SNR values of -3 dB or lower, the number of measurements that can be used in localization has improved on average by $15-20\%$ in LOS and $20-30\%$ in NLOS cases. This implies that by using wavelet de-noising we were able to improve not only the detectability of the signal but the detectability of the first peak too. It has also been shown that the RMSE for those measurements that are within the usable range error, increases after de-noising. This implies that, while de-noising has increased the number of measurements that can be used for localization, the average error of those measurements has increased slightly. Thus, there is a trade off between the number of usable measurements and the accuracy that comes with that.

There is also another way of looking at the advantage obtained by improving the SNR. If you know the noise level of your environment, by using wavelet de-noising at the receiver side, it is possible to transmit your signal with less power. In other words, wavelet de-noising enables us to lower the transmission power.

However, de-noising also has a negative effect under high SNRs resulting in an increased range error. As such, the number of measurements that are within the usable range has decreased at high SNRs. Also, for similar reasons, at high SNRs, the RMSE has increased.

Chapter 3

CHANNEL IDENTIFICATION

Provided the sensors are in LOS, ToA ranging can provide cm level accuracies. This is possible because of the presence of the direct paths. However, in the case of OLOS/NLOS, there is an obstacle between the nodes. Depending on the type of obstacle, the direct path is either delayed or it is completely blocked. If it is blocked, only reflections from nearby objects will be received. Figure 3.1 shows the three possible situations: Receiver 1 is in LOS, Receiver 2 is in OLOS, and Receiver 3 is in NLOS.

In both the OLOS and NLOS case, a bias is introduced in the range estimate, making it less accurate. Thus, for those sensors that are in NLOS there is a need to mitigate the error introduced by the obstacles/reflectors. However, before doing mitigation it is important to identify if the target node is in LOS or not, as mitigation has to be applied only to those sensors that are either in OLOS or NLOS.

Channel identification is also important from the perspective of localization. For instance, in the case of trilateration based localization there is a need for three range estimates in order to localize the node in a 2D space, as explained in Chapter 1. In doing so, because of the high accuracy and precision present in the LOS ranging, it is preferable that all the three range esti-

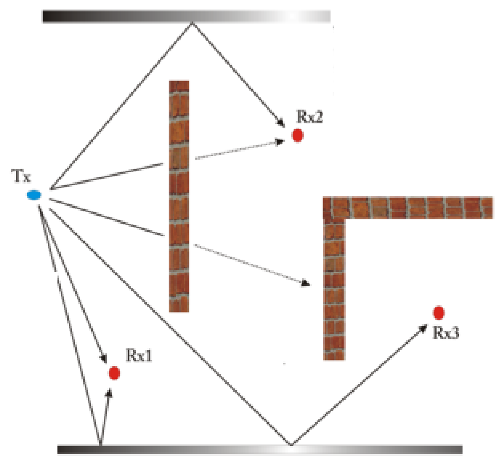

Figure 3.1: LOS (Rx_1), OLOS (Rx_2), NLOS (Rx_3) situations

mates are done by reference nodes that are in LOS with respect to the target node. NLOS range estimates are to be used only in the absence of enough LOS measurements. Thus, there is a need to exactly identify whether the range estimate is made by a LOS or NLOS reference node. In some cases, NLOS range estimates can also be used in assisting LOS measurements. Even in those cases, the need for identification still persists.

In [17], the issue of classification was approached using a ray tracing algorithm. This algorithm requires knowledge of the map of the environment. Moreover, the computational complexity that comes with it is high. Other papers have addressed the classification problem from a statistical features perspective. Characteristic features extracted from the received signal can provide us with information about the scenario. Kurtosis, a feature to be explained later, is used as a feature for classifying LOS and NLOS situations in [20]. This technique was tested using the 802.15.4a channel model and had a success rate of 74%. Moreover, in [21, 26] statistical features extracted from the received waveform are used for classification. In those cases, mean excess delay, rms delay and kurtosis are used. A comparison is made between using the features individually or using them jointly. The technique was evaluated using simulations and success rate over 90% was obtained for most of the environments. However, in those cases, the threshold selection for decision making is not clearly defined. Similar techniques are also used in [22] different feature combinations are tested and among them excess delay, rise time, and kurtosis are chosen. Using the opted features with SVM classifier, this mechanism had more than 90% success rate with actual measurements.

Op 't Land [52] proposed a mechanism where nodes are selected not based on the channel state (LOS/NLOS), but based on the estimated range error. To do so, first a fitting function was estimated between the range error and the characteristic features. This fitting function was approximated using an arctan (inverse tangent) curve. Accordingly, the characteristic features are used to estimate the range error, and, eventually, the nodes with the lowest estimated ranging error are used in localization. In other words, nodes with low ranging errors are assumed as if they are in LOS. This would be true if the relation developed between features and the ranging error were exact and the arctan curve fitted the data accurately. However, in this thesis, there are a number of outliers to the fitted curve. The data are so scattered and diverse, that it is hard to realize a relation between the range error and features. Referring to the results of Op 't Land given in Figure 6.16 of his thesis, a number of measurements with low range error are estimated to have large errors. Also, a number of measurements with high range error are also estimated to have low range error. Thus, the results were not convincing.

In our case, we will address the identification problem from a characteristic features perspective. In Figure 3.2 the parts of the flow chart addressed in this chapter are indicated in the highlighted box. We will investigate a robust and at the same time simple classification technique. The overall aim is not only to identify LOS and NLOS but to do so with less complex algorithms. The complexity of the classification technique will highly depend upon what features are used. Hence, an extended list of features will be analyzed and examined. Looking at the relation between the features and the scenarios (LOS/NLOS), the most appropriate features will be selected. Ultimately, those features will be used along with a simple classification algorithm in determining if a target node is in LOS or not. Evaluation of the technique is going to be based on actual measurements.

Accordingly, the first section is going to deal with features and their detail characteristics. Why and how those features can assist in classification is explained in this section. The extraction of those features from actual measurements and their analysis is done in Section 3.2. The selection of the most promising features is also done in this section. Details of the classification algorithms are discussed in Section 3.3 while their evaluation with respect to the actual measurements is done in Section 3.4. Conclusion of the work done in this chapter is presented in Section 3.5.

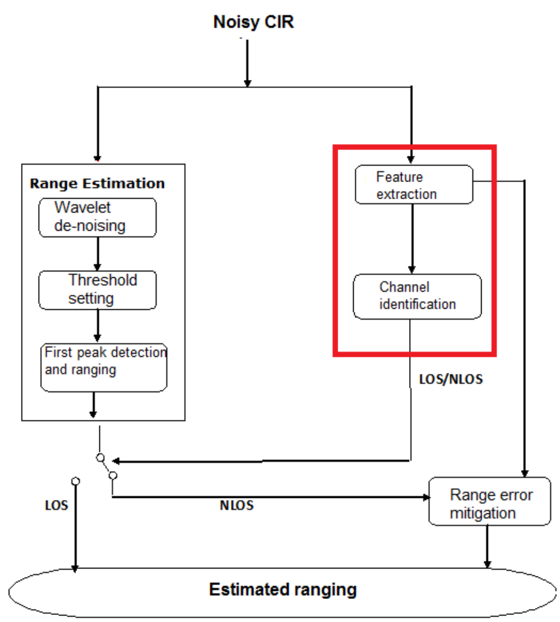

Figure 3.2: Ranging Approach, flow chart

3.1 Impulse response features and characteristics

Features that can be extracted from an impulse response are broadly grouped into two as *time statistics based* and *amplitude statistics based* features. Detailed definition and formulation of these features is presented in this section. These features are also going to be used in the mitigation techniques in Chapter 4.

3.1.1 Time statistics based features

Time statistics based features indicate the distribution of the channel impulse response (CIR) with respect to time. The features analyzed are mean excess delay, RMS delay, rise time, and global peak delay.

Mean excess delay

The mean excess delay ($\mathscr{T}_{\mathsf{e}}$) is the first moment of the path delay with respect to the estimated first path using the power delay profile as a weighing function. Mathematically, this is expressed as

$$\mathscr{T}_{\mathsf{e}} = \frac{\sum_{m=1}^{M} |h_{\mathrm{b}}[m]|^2 . \left(\frac{m-1}{f_s} - t_0\right)}{\sum_{n=1}^{N} |h_{\mathrm{b}}[m]|^2} \tag{3.1.1}$$

where f_s is the sample rate, t_0 is the delay of the first path, m is the number of samples and h_{b} is the sampled base band CIR. The mean excess delay has been used in literature for quite some time [21, 22, 26], and it has proven to be one of the useful features in both identification and mitigation techniques.

Both in in the case of obstructed line of sight or absence of line of sight, the mean excess delay will be larger than in the LOS situation. Moreover, this parameter could also give us an idea about the type of environment. The presence of scattering objects in close proximity (which could be the case in indoor office/residence) is likely to result in a smaller mean excess delay than in a situation where the objects are located at a distance, like in outdoor environments.

RMS delay spread

RMS delay is a measure of the temporal dispersion of the multipaths and is defined as the square root of the second central moment of the path delay. Mathematically,

$$\mathcal{T}_{\mathtt{RMS}} = \sqrt{\frac{\sum_{m=1}^{M} |h_{\mathrm{b}}[m]|^2 . \left(\frac{m-1}{f_s} - t_0 - \mathcal{T}_{\mathtt{e}}\right)^2}{\sum_{m=1}^{M} |h_{\mathrm{b}}[m]|^2}} \tag{3.1.2}$$

Rise time

Rise time is the time difference between the instant at which the channel impulse response (CIR) first exceeds certain per-specified values. Quantitatively, this is given by

$$t_{\mathrm{rise}} = t_H - t_L, \tag{3.1.3}$$

where

$$t_{\mathrm{H}} = \min\{t : |h_{\mathrm{b}}[m]| \geq \alpha\sigma_{\mathrm{n}}\}$$

$$t_{\mathrm{L}} = \min\{t : |h_{\mathrm{b}}[m]| \geq \beta \max(|h_{\mathrm{b}}[m]|)\}$$

While σ_{n} gives us the noise level, α and β are constants chosen to define the rising edge. Typical values are 6 and 0.6 respectively.

Global peak delay

The global peak delay is the time difference between the global peak and the first peak. In LOS situations, the first peak is usually the global peak. As such, the global peak delay is expected to be around zero for LOS. In NLOS however, it is expected to have a higher value. This feature is going to have a relative significance in deciding whether a target node is in LOS/NLOS.

3.1.2 Power features

Power based features give information regarding the distribution of the values of the CIR. The features analyzed are kurtosis, ricean K factor, number of significant paths, maximum of the received signal and energy of the received signal.

Kurtosis

The kurtosis is a statistical parameter that indicates the centralized fourth order moment of the normalized CIR amplitude. Kurtosis, unlike the previous features, is a measure of the amplitude spread of the received signal, showing how peaky the signal is, i.e. to what extent the variance is determined by relatively large values. The mathematical definition of kurtosis is given by

$$\mathcal{K} = \frac{\sum_{m=1}^{M}\left(|h_b[m]| - \overline{|h_b[m]|}\right)^4}{\left[\sum_{m=1}^{M}\left(|h_b[m]| - \overline{|h_b[m]|}\right)^2\right]^2} \tag{3.1.4}$$

where $\overline{h_b[m]}$ is the mean of the base band CIRs.

Normally, kurtosis is expected to be larger for LOS than for NLOS. In the case of NLOS situations, kurtosis is also anticipated to show variation depending on the type of obstacles and scatterers present.

Kurtosis has been used as one of the features for identification and mitigation in localization in [21, 22, 26, 34]. Moreover, kurtosis has also been used in [35], in estimating the ToA. Based on those papers, kurtosis is a powerful feature in identifying LOS from NLOS.

Ricean K factor

The ricean K factor is the ratio between the power in first path and the power in the scattered paths:

$$R_k = \frac{|h_b[m_0]|^2}{\sum_{m=(m_0+1)}^{M} |h_b[m]^2} \tag{3.1.5}$$

where m_0 is the sample signaling the first peak. Under LOS conditions, this is going to be the ratio between the direct path and the rest of the received paths. Comparing this with the NLOS condition, we expect to have a higher ricean K factor, because in NLOS situations the direct path is either obstructed and thus attenuated or not present.

Number of significant paths

The number of significant paths could be defined as the minimum number of paths that make up, say, 85% of the total power of the received signal. 85% is the value that was used in [36], but it is not a hard number and as such is subject to changes. In our case, we are using the same definition, i.e. 85 % of the total power of the received signal.

This feature can help us in further identifying LOS and NLOS. In LOS situations, because of the presence of a direct path, it is expected that the total number of paths that make up 85% of the total power of the received signal is going to be less than that of NLOS.

We have an alternative definition of number of significant paths. This is defined as the number of paths that are within, say, 10 dB of the strongest path. This is another way of looking at the feature, though again, we expect NLOS to have more significant paths than LOS.

For our analysis both features will be investigated and their significance will be examined.

Maximum of the received signal

The maximum of the received signal is nothing but the global peak. At this stage, what we compare is the amplitude/power rather than the delay of the peak, which is the case in the global peak delay feature. In the LOS cases, because of the direct and unobstructed path between the receiver and transmitter, we expect to have a higher peak than those of NLOS/OLOS. Coincidental, it is possible that a constructive combination of multipaths could cause the peak of the NLOS to be more than what that of LOS.

Energy of received signal

This feature is going to measure the total energy of the received signal. Normally, in the case of NLOS/OLOS, because of obstructions and reflections, the energy of received signal is expected to be lower than in LOS scenarios.

3.2 Characteristic features based on NIST measurements

In order to verify our analysis, features were extracted from actual measurements (NIST measurements). As is mentioned in the previous chapter, those measurements were done in four environments namely: north, child care, sound and plant. In each environment there are 10 measurements that are in LOS and 40 in NLOS.

Figures 3.3 and 3.4 show the features for the four environments. All the measurements are grouped together and a histogram of both LOS and NLOS measurements is made. The idea is to make an eye inspection on whether a given feature can be used to separate LOS and NLOS measurements.

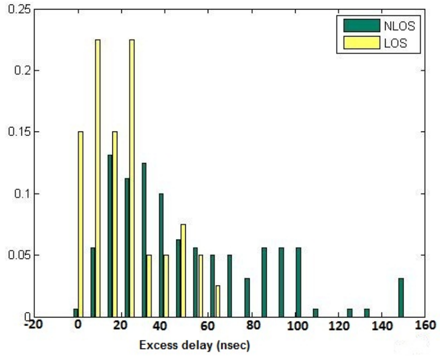

(a) Excess delay

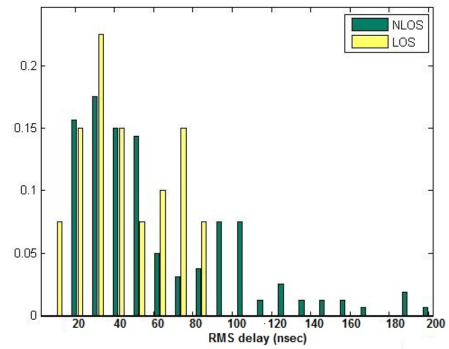

(b) RMS delay

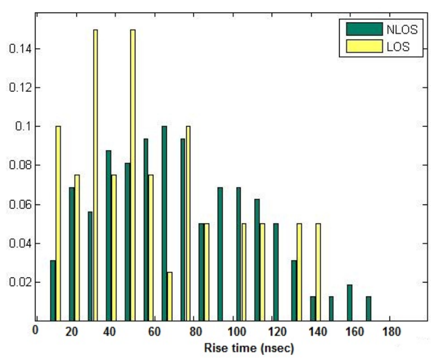

(c) Rise time

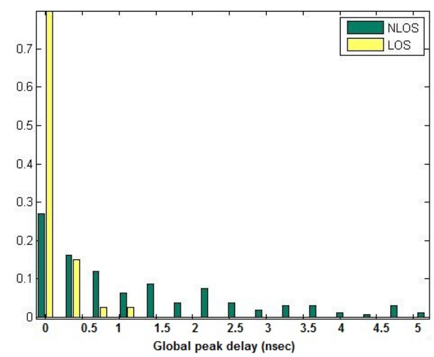

(d) Global peak delay

Figure 3.3: Histogram plots of the time based features

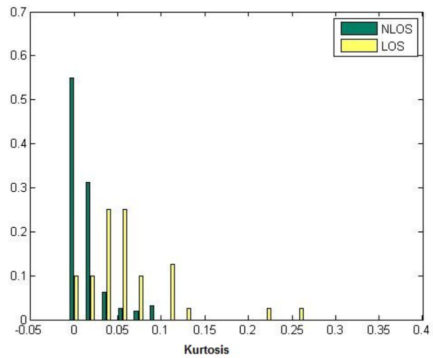

(a) Kurtosis

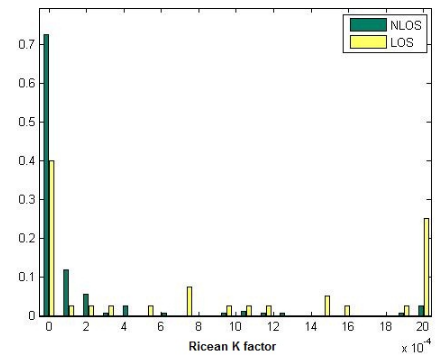

(b) Ricean K factor

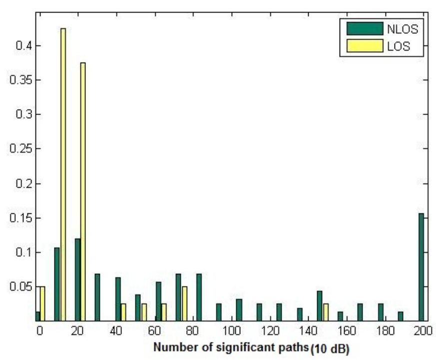

(c) Number of significant paths (10 dB)

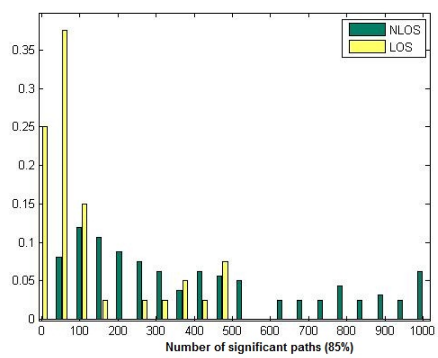

(d) Number of significant paths (85%)

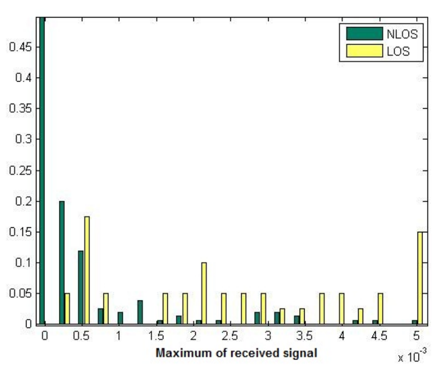

(e) Maximum of received signal

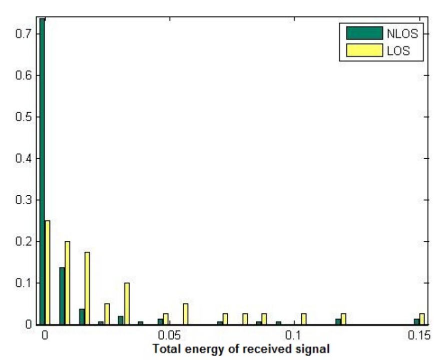

(f) Total energy of received signal

Figure 3.4: Histogram plot of the power based features

Looking at the figures, it is clear that none of the features can be used individually for channel identification. This is because in all the features there is an overlap between the LOS and NLOS measurements. Nevertheless, we can use a combination of features to come up with a relation that will assist us in the identification process. As predicted, the trends discussed in Section 3.1.1 and 3.1.2 hold for most of the features. However, no clear distinction could be made between the LOS and NLOS when referring to rms delay, rise time and ricean K factor. That is, in those cases, there is a large overlap between LOS and NLOS, making it difficult to make a clear cut.

In the rest of the features, the area of overlap is smaller compared to the previous ones. Hence, we have selected excess delay, kurtosis, global peak delay, number of significant paths (85%), number of significant paths (10 dB), maximum of received signal, and energy as the features to be investigated for identification.

3.3 Statistical classifiers

In the previous section we have identified the features that might assist us in channel identification. However, the question of how those features should be used collectively and whether all the features are relevant or not is still to be answered.

One way of using the features collectively is to use a weighting scheme, where weights are assigned to each feature. The weight assignment depends on how a given feature is relevant for classification. Ultimately, those features with the higher weights will greatly influence the decision making. In our case, those features with less overlap between LOS and NLOS would have larger weights compared to those with higher overlap between LOS and NLOS. The question here is how to assign the exact weight value to each feature.

Fortunately, we have a mechanism to do that: machine learning based classifiers. In those techniques, what happens is that the data are separated into two, as training set and testing set.

For the training sets, we already know whether they are in LOS or NLOS. Because we know the scenario (LOS/NLOS), weights could be set to give optimal result. Different machine learning classifiers use different mathematical tools to come up with a weight that will give the best result for all the training data set.

Once the weights are set based on the training set, we need to make sure whether the weights work fine with all the measurements. Therefore, the testing set is used. Using the same weights as those of the training set, the testing set is examined. Accordingly, the accuracy of the technique is measured by its success rate for the testing set.

In our case, we are going to investigate both the simple and high level classifiers. We will see if the success rate of our identification depends on the complexity of the classifier used. While there are a number of classifiers present, the simplest ones are linear classifiers. Among the linear classifiers, the *Naive Bayesian* classifier stands out in practical applications.

The Naive Bayesian classifier is well known because of its simplicity, computational efficiency and its surprisingly good performance for real-world problems. The naive Bayesian classifier works under the assumption that the features are independent i.e. the value of a given feature is not dependent on the values of the other features. In our case, this is a subtle argument. To a certain extent the features are correlated. In spite of serious violations of the basic assumptions and the simplistic design of the classifier it turns out that they are very well suited for real problems. For instance most email clients such as Mozilla Thunderbird or Microsoft Outlook use Naive Bayesian classifiers for filtering out spam emails.

In order to assess the success rate and failure of the Naive Bayesian classifier, it is necessary to compare it to other complex classifiers. This is done in order to quantify the loss obtained by using simple classifiers or the gain that would have been obtained, if a more complex algorithms were used. This indirectly would also give us an indication on how relevant the features are. Therefore, an *SVM* classifier is used for comparison.

SVM classifiers are more complex but at the same time they are extremely powerful. SVM is a powerful methodology for solving problems in nonlinear classification, function estimation and density estimation which has also led to many other recent developments in kernel based methods [58]. In [59, 60, 61, 62], details of SVM classifiers are explained. SVM classifiers are based on the idea that, by increasing the dimensionality of the data, it gets easier to separate. In fact, the SVM uses an N-dimensional space, where N is the number of samples in the training set. This approach allows the SVM to classify problems with arbitrary complexity. In our case we are going to use least square based SVM (LSSVM). This is more general and efficient as it tries to solve a list of linear equations rather than quadratic ones. As is mentioned in [63], for a binary classification the accuracy of LSSVM is equivalent to nominal SVM, as such by using LSSVM we are reducing the complexity while not affecting the accuracies of the results.

3.4 Statistical classifiers for channel identification

In the previous sections, two types of classifiers and the features that are to be used for classification have been presented. In this section we will apply those classifiers on the features and see their success rate.

As is previously mentioned, we have 40 measurements in LOS and 160 in NLOS. Around 60% of the measurements (110) are used for training while the rest (90) are used for testing the classifier. Moreover, the question of exactly how many features to use and which ones is yet unanswered. Thus, we have analyzed all possible combinations between the selected features. Table 3.2 give the most relevant results for the features extracted from the original NIST measurements i.e. without adding noise or de-noising them.

The results given are for both Bayesian and SVM classifiers. The success rate obtained from both classifiers was the same i.e. the results did not depend up on the type of classifier but more on the type of features used. Taking the simplicity and computational efficient in to account, the Bayesian classifier is opted over SVM classifiers.

As can be inferred from the Table 3.3, the best result is obtained when kurtosis and number of

Table 3.1: Characteristic features based channel identification (missed detection is when a node in NLOS is wrongly detected as LOS and false alarm is when a node is LOS is falsely detected as NLOS)

Missed detection	False alarm	Features
1.1%	8.8%	energy, rise time and $\mathscr{K}$
0%	11.1%	energy, global peak delay and $\mathscr{K}$
0%	0%	energy, global peak delay, $\mathscr{K}$ and sig (80%)
0%	0%	$\mathscr{T}_{\mathsf{e}}$, global, $\mathscr{K}$ and sig (80%)
2.2%	0%	sig(80%)
0%	0%	sig(10dB) and $\mathscr{K}$
0%	3.3%	sig(80%) and global peak delay
0%	3.3%	sig(80%) and $\mathscr{T}_{\mathsf{e}}$
1.1%	0%	sig(80%) and energy
0%	0%	sig(80%) and $\mathscr{K}$

significant paths is used. When a combination of both features is used we have a 100% success rate.

In the previous chapter we have presented the importance of wavelet de-noising for first peak detection and how it can help us decrease the error in ranging. The question is then whether noise affects the identification technique and what the effect of de-noising is on channel identification. Therefore, we have extracted both kurtosis and the number of significant paths (85%) from the signals before and after de-nosing and examined the success rate using the Bayesian and SVM classifiers. Table 3.2 gives the error probability before de-noising and Table 3.3 gives the error probability after de-nosing. The training data was established from the noise free measurements. Note that, in the cases where the signal was undetectable, all the features were set to zero.

Table 3.2: Characteristic features based channel identification before de-noising

SNR	Error Probability before de-nosing					
	Linear classifier			SVM classifier		
	P_f	P_m	P_e	P_f	P_m	P_e
−12 dB	10%	82.2%	46.1%	0%	80%	40%
−9 dB	7.8%	76.6%	42.2%	0%	77.7%	38.9%
−6 dB	10%	74.4%	42.2%	0%	65.5%	32.8%
−3 dB	8.9%	64.4%	36.7%	0%	44.4%	22.2%
0 dB	8.9%	48.8%	21.7%	0%	27.8%	14%
3 dB	7.8%	18.9%	28.3%	0%	23.3%	11.7%
6 dB	2.2%	14.4%	8.3%	0%	18.4%	9.2%
9 dB	2.2%	8.9%	5.55%	0%	8.8%	4.4%
12 dB	2.2%	6.67%	4.5%	0%	6.7%	3.4%

Table 3.3: Characteristic features based channel identification after de-noising

SNR	Error Probability after de-nosing					
	Linear classifier			SVM classifier		
	P_f	P_m	P_e	P_f	P_m	P_e
−12 dB	2.2%	80%	41.1%	0%	80%	40%
−9 dB	2.2%	77.7%	39.5%	0%	80%	40%
−6 dB	7.8%	72.2%	40%	0%	75.5%	37.75%
−3 dB	7.8%	72.2%	40%	0%	75.5%	37.75%
0 dB	8.9%	44.4%	26.4%	0%	48.8%	24.4%
3 dB	10%	20%	15%	0%	23.3%	11.65%
6 dB	10%	14.4%	12.2%	0%	16.7%	8.35%
9 dB	10%	8.9%	9.45%	0%	12.2%	6.1%
12 dB	7.8%	5.5%	6.65%	0%	6.67%	3.34%

Assuming that LOS and NLOS are equally likely, the mean error probability is given by

$$P_\mathrm{e} = \frac{P_\mathrm{f} + P_\mathrm{m}}{2} \tag{3.4.1}$$

Referring to Table 3.2, noise has greatly affected the identification process. It is shown that SVM out performs the linear classifier, as expected. However, the results seem to have more of a random nature. Thus, the one thing that can be concluded from the results is that both noise and de-noising affect the identification process.

3.5 Conclusion

In this chapter, the idea of channel identification and its necessity are addressed. Various characteristic features are extracted from the received signal, to analyze if they can assist in the identification process. Though none of the features examined can be used individually for identification, a combination of those can give us a better result. Specially, a combination of number of significant paths and kurtosis has shown to be reliable. Naive Bayesian and SVM classifiers have been used for classification. Both mechanism have led us to the same result.

Looking at the complexity of the features involved, the number of significant paths (85%) requires re-ordering of the samples. Compared to the number of significant paths (10dB), this will have more computational complexity. Thus, the latter one is proffered.

It can also be concluded from this chapter that, noise does affect the identification process adversely. Even after de-noising the measurements, the identification process performs poorly. Therefore, based up on our results, it is suggested to have a more customized identification technique, i.e. an identification technique that is SNR dependent.

Nevertheless, the main objective of this chapter was to develop a classification technique that is robust and simple. This has been made feasible with the help of kurtosis and number of significant paths. These features are found to be the most relevant features in classification. Regardless of the complexity of the classifier used, as long as both features are the only ones used, then the success rate of the classifier has been 100%.

Chapter 4

RANGE ERROR MITIGATION

In the previous chapters, we have been able to estimate the range of a sensor with respect to another sensor. Moreover, with high certainty we could identify which of the sensors are in LOS and which are not.

One thing that is made clear from the earlier treatments of ranging is that *there is a positive bias in the range estimate of a NLOS sensor.* The bias introduced will results in an error in the range estimate. This is explained in Figure 3.1. In such cases, there is a need to mitigate the error introduced. This is the subject of this chapter; see Figure 4.1.

While different papers treat this problem differently, most of them try to estimate the range error and ultimately deduct it from the range estimate. The most common research method is the statistical feature based mitigation, where features are extracted from the CIR. Those features are used for estimating the error in ranging. In [26], kurtosis, mean excess delay and rms delay spread are used for estimating the range error. Different weights are given to each feature, and, accordingly, the optimal weights are selected. In [27] mean excess delay, power of the first peak and the total power of the CIR are used to estimate the range error. The paper shows almost 50% decrease of the root mean square error after mitigation, in the NLOS cases. The last two papers assume that the statistics are the same for different environments, which is not valid always as the characteristic features vary depending on the environment.

Op 't Land [52], has approached the mitigation using a fitting curve algorithm. A fitting curve technique was used for establishing a relation between a certain feature and the range error. This was done for all features analyzed. Accordingly, a weight was given to each feature and Naive Bayesian was used for regression. Naive Bayesian regression assumes that the features involved are not correlated. However, some of the features used in the paper are highly correlated, like coherence bandwidth and rms delay. Thus, those assumptions could possible degrade the overall performance of the regression process.

In our case, initially, nodes in LOS and NLOS are distinguished. This is treated in detail in the previous chapter. For those measurements that are in NLOS, a relation is established between the error in ranging and the various characteristic features. This is done to investigate which features highly correlate with the range error. Accordingly, out of all the features, the most relevant ones are selected. Once this is done, a regression technique is used. One of the most powerful regression techniques is *SVM regression*. This technique assumes a non-linear relation between the features and range error. This technique is used in our case.

In Section 4.1 an investigation is made on the relation between each feature and the range error. This is done with the help of correlation coefficient. Accordingly, the most correlated features are selected. Following a brief discussion on the regression techniques used, in Section 4.2, the range error before and after regression is analyzed. In all the analysis, the NIST measurements discussed in Chapter 2 are used.

4.1 Characteristic features and ranging error

In Chapter 3, the following features were dealt with: mean excess delay, RMS delay, kurtosis, rise time, ricean factor, global peak delay, number of significant paths (85%), number of signif-

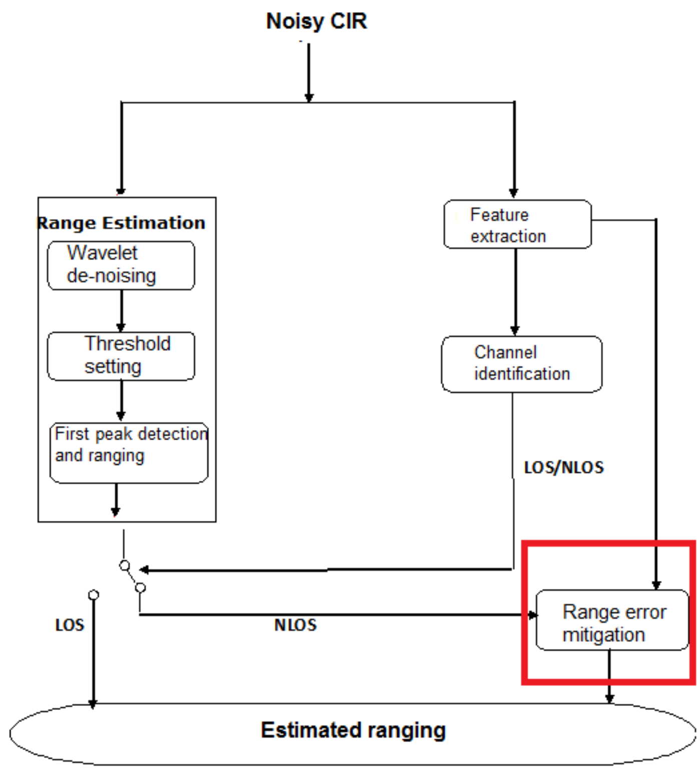

Figure 4.1: Problem flowchart

icant paths (10 dB), energy of the received signal, and maximum of received signal. In order to investigate if those features can assist in estimating the ranging error, a correlation coefficient has been calculated between the features and the range error. The idea is to asses which of the features are more related to the error in ranging.

One additional feature that has been included in the set is the *range estimate*. As noted in [22], the ranging error tends to increases with increasing distance, making it a relevant feature for mitigation. Therefore, this feature is also included in our analysis.

Looking at Table 4.1, in relative terms, for all the buildings the *mean excess delay*, *global peak delay* and *range estimate* give a large correlation coefficient, making them the most relevant features to use for mitigation.

In order to investigate the impact of the *range estimate* on mitigation, we will analyze regression with and without it.

Table 4.1: Correlation Coefficient between features and ranging error

Features	Correlation Coefficients			
	North	Child Care	Sound	Plant
Mean excess delay and Range error	0.56	0.72	0.79	0.37
RMS delay and Range error	0.44	0.73	0.39	−0.14
Kurtosis and Range error	−0.14	−0.33	−0.36	−0.3
Global peak delay and Range error	0.52	0.51	0.78	0.49
Sig(80%) and Range error	0.43	0.39	0.39	0.1
Sig(10dB) and Range error	0.51	0.68	0.49	−0.05
Range estimation and Range error	0.56	0.77	0.82	0.55
Energy of received signal and Range error	−0.17	−0.34	−0.14	−0.34
Maximum of received signal and Range error	−0.13	−0.36	−0.26	−0.41

4.2 Range error estimation

To estimate the ranging error, a regression technique is used. Unlike the classification technique (Chapter 3), regression requires many training samples, in the order of hundreds.

SVM is used for regression in [22, 59]. As explained in [59, 60, 61], SVM regression is quite powerful. However, SVM requires high training samples. Its accuracy does not only depend on the type and number of features used but also on the number of training samples used. Looking at the efficacy and accuracy of SVM regression, it is used in our analysis.

SVM regression is highly complex, but, as it is done offline, its complexity hardly has an impact on the sensor network. For the purpose of regression we have used an SVM tool developed by the *Katholieke University of Leuven*, Belgium [65]. The tool was developed to make an effective and easy usage of LSSVM. It incorporates various SVM algorithms used for classification, regression and unsupervised learning.

4.2.1 Regression using SVM

In order to test whether the ranging error can be estimated using the selected features, SVM regression is used. Out of the 160 NLOS measurements, 100 of them are used for training, while the rest (60) are used for testing.

Figure 4.2 shows the error in ranging before and after regression. The figures gives two plots after regression, one with the initial range estimate incorporated and the other without incorporating the initial range estimate.

When using the initial range estimate as one of the features, the maximum ranging error is improved with the help of SVM regression i.e. the maximum range error is reduced from about 12.5 m to 11 m. However, no improvement is seen when considering only range errors that are less than 1m.

On the other hand, when the range estimate is not used in the features, the number of measurements that are within 1 m in range error has improved from around 50% to 60%. The maximum error has also reduced to around 10 m.

Comparing the root mean square error in the three situations results in 6.7 m before regression, 2.8 m after regression with initial range estimate incorporated and 3.2 m after regression but when initial range estimate is not incorporated. That is, the RMSE has decreased by 59% when using the range estimate as one of the features, while it has decreased by 53% when it is not included in the list of features used for regression.

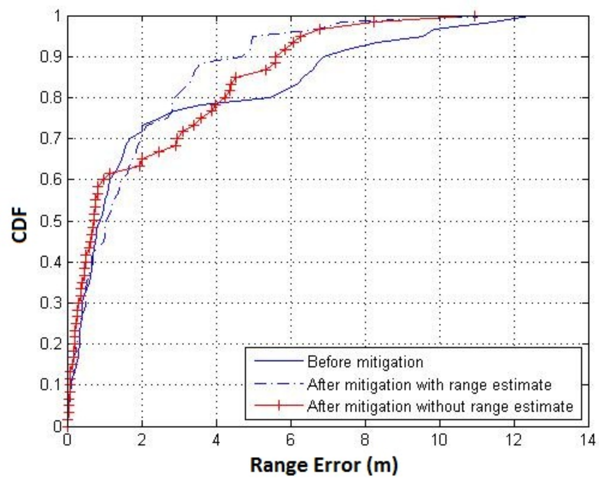

Figure 4.2: CDF of range error before and after SVM regression

In order to see what is going on with the individual measurements, Figure 4.3, plots the the range error before and after regression. In this case, range estimate is used as one of the features.

In Figure 4.3, Region I, is where the range error has increased after regression, while region II is where regression has reduced the range error. As can be seen from the figure, large errors are decreased using regression. This is the reason for the more than 50% decrease in RMSE. On the hand, the small range errors are increased by using a regression technique.

Regression is the last step in most ranging algorithms. That is after mitigating the range error using regression, then the measurements should be usable for localization. In Chapter 2, we have assumed that to have a cm level of accuracy in localization, it is necessary that the individual range errors should not be more than 1 m. Using this assumptions, the results shown no significant improvement.

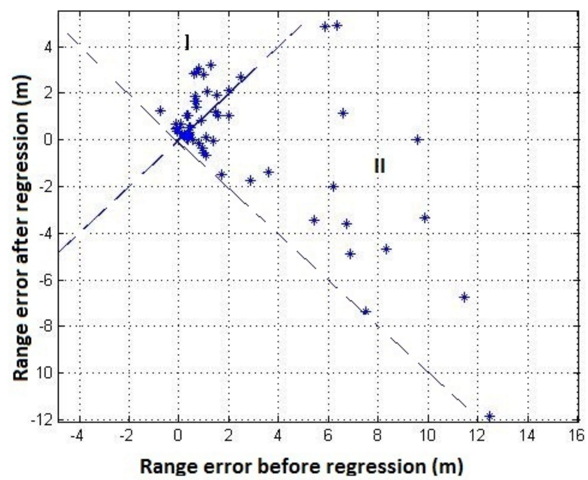

Figure 4.3: Range error comparison before and after regression

4.3 Conclusion

In this chapter, we have shown that there is correlation between the error in the range estimate and features like range estimate, global peak delay and excess delay. In [52] the range estimate is not used as one of the features for regression, but, its importance in regression has been pointed out in this chapter. When using the range estimate as one of the features, the RMSE decreased by almost 60%.

It has also been shown that regression techniques affect the small error adversely, causing an increase in the range errors. However, if the initial range errors are large, then regression can help in decreasing the range error. Based on our results, the number of NLOS measurements that can be used in localization did not change after regression.

However, it is important to note that those results were obtained with very limited number of training samples, only 100. As in all regression techniques, the efficiency of SVM regressors depend on the number of training samples you have. The more trainers you have the better result you might get. Thus, may be, a better performance could have been obtained if there had been more training samples.

In our case, all the NLOS measurements were used together. However, it seems that a more customized (in our case, north, sound, child care and plant) regression technique could be more robust and accurate. That is, if a regression technique are developed separately for those measurements done in a specific environment, the result could have been more accurate. For instance, there is a high correlation between the selected features and the error in ranging, in the case of north building while the correlation is small in the case of plant.

However, the level of accuracy and the mechanism needed to do a customized approach are left for further research, since in our case, the number of measurements we have are limited to do such analysis.

Chapter 5

CONCLUSIONS AND RECOMMENDATIONS

This thesis provides an analysis of the ToA ranging problem and investigates ways to overcome the current limitations of this technique. The overall conclusion of the work, followed by possible future extensions is provided in this chapter.

5.1 Conclusion

We started off this thesis with three research questions:

1. Can we improve the range estimate in low SNR situations ?
2. Can we exclusively identify sensors in LOS from those in NLOS?
3. Can the ranging errors in NLOS be estimated and mitigated?

Looking back at the analysis and results of this thesis, the following conclusions are drawn.

The ranging error associated with ToA ranging depends on the SNR and the bandwidth of the signal. Thus, improving the SNR can have a direct result in improving the ranging errors in both the LOS and NLOS scenarios. In this case, wavelet based thresholding was investigated. In situations where the signal was totally buried under the noise, wavelet de-noising has improved the detectability of the signal and ultimately the first peak. Detectability of the signals has increased on average by 20−30% while the number of measurements that are within 1 m in range error has increased on average by 10−15%, depending on the SNR.

Characteristic features extracted from the CIR can provide us with quite a lot of information. By using characteristic features it is possible to distinguish between those nodes in LOS and those in OLOS/NLOS with a high degree of accuracy. When just the kurtosis and the number of significant paths are used, the success rate in channel identification was 100%. This is true with both the complex classifiers like SVM and the simple classifiers like the Naive Bayesian classifier. However, when noisy CIRs the performance of the identifier is greatly degraded. Even after de-noising the performance is adversely affected. Under such cases, an identification technique that is SNR dependent could provide us with better results.

In order to mitigate the ranging error in the case of OLOS/NLOS situations, sophisticated regression techniques are needed. For this purpose, regression techniques like LS-SVM and robust SVM can be used. However, those techniques require a large number of training samples, and so, a large measurement database is required if those techniques are to be exploited effectively. In our case, LS-SVM regression was used. Among the various features analyzed, excess delay, global peak delay and range estimate have high degree of correlation with the range error. Using those features along with LSSVM, the maximum error in ranging was reduced from 12.5 m to about 7m, while the RMSE was decreased by almost 50%. However, no improvement was seen when considering the number of measurements that are within 1 m in range error.

5.2 Recommendations

The analysis and assessments done in this thesis are mainly based on limited number of measurements. Simulations based on the IEEE 802.15.4a channel models are used when deemed necessary. Doing a large number of measurements, in different environments could make the results more conclusive. The IEEE 802.15.4a channel model is limited from ranging and localization perspective. The absence of actual distance information greatly limits the usage of the model for positioning. That is, the model needs to be updated from the localization point of view, and, most importantly, it should provide information regarding the relation between the features and the actual distance between the nodes.

Regarding the mitigation techniques, our results were limited due to the low number of measurements present. More measurements would have provided more reliable results. This is because, SVM trainers require hundreds if not thousands of trainers.

Customized regression could improve the mitigation technique. The idea is to develop a regression technique that is specific to a given environment. Environments could be classified depending on the characteristic features and the error in ranging. Then, for each environment, a more tailored regression technique could be developed. Similarly, the analysis of a more customized (i.e. SNR dependent) classifier is left for further research.

Bibliography

[1] K. Pahlavan, X. Li, and J. Makela, “Indoor geolocation science and technology,” *IEEE Communications Magazine*, vol. 40, no. 2, pp. 112,– 118, Feb. 2002.

[2] C. C. Chong, I. Guvenc, F. Watanabe, and H. Inamura, "Ranging and Localization by UWB Radio for Indoor LBS," *NTT DOCOMO Technical Journal (English version)*, Vol. 11, No. 1, pp. 41-48, June 2009

[3] Hui Liu, H. Darabi, P. Banerjee, and Jing Liu, "Survey of Wireless Indoor Positioning Techniques and Systems," *IEEE Transactions on Systems, Man, and Cybernetics, Part C: Applications and Reviews,* vol. 37, no. 6, pp. 1067−1080, Nov. 2007.

[4] B. D. Van Veen and K. M. Buckley, “Beamforming: A versatile approach to spatial filtering,” *IEEE ASSP Mag.*, vol. 5, no. 2, pp. 4–24, Apr. 1988.

[5] P. Stoica and R. L. Moses, *Introduction to Spectral Analysi*s, Englewood Cliffs, NJ: Prentice-Hall, 1997.

[6] B. Ottersten, M. Viberg, P. Stoica, and A. Nehorai, “Exact and large sample ML techniques for parameter estimation and detection in array processing,” *in Radar Array Processing*, S. S. Haykin, J. Litva, and T. J. Shepherd, Eds. New York: Springer-Verlag, 1993, pp. 99–151.

[7] A. F. Molisch, K. Balakrishnan, D. Cassioli, C.C. Chong, S. Emami, A. Fort, J. Kared al, J. Kunisch, H. Schantz, U. Schuster, and K. Siwiak, “A comprehensive model for ultrawideband propagation channels,” *in Proc. IEEE Global Commun. Conf.*, Mar. 2005, pp. 3648–3653.

[8] R. Szewczyk, “UWB: Technology and implications for sensor networks”, *NEST Meeting,* 2004.

[9] W. Vereecken, M. Steyaert, “Ultra-Wideband Pulse-based Radio,” *Reliable Communication over a Wideband Channel Series,* 2009.

[10] Young Man Kim, “Ultra wideband (UWB) Technology and Applications,” *Ohio State University, NEST group.*

[11] L. E. Miller, “Why UWB? A Review of Ultra-wideband Technology,” *NIST WCTG report,* April 2003.

[12] Camillo Gentile, Sofia Martinez Lopez, Alfhighlighted Kik, “A Comprehensive Spatial-Temporal Channel Propagation Model for the Ultra-Wideband Spectrum 2-8 GHz,” *GLOBECOM,* 2009.

[13] S. Gezici, Zhi Tian, G. B. Giannakis, H. Kobayashi, A. F. Molisch, H. V. Poor, and, Z. Sahinoglu, "Localization via ultra-wideband radios: a look at positioning aspects for future sensor networks," *IEEE Signal Processing Magazine*, vol.22, no.4, pp. 70-84, July 2005.

[14] G. Bellusci, G. Janssen, Junlin Yan, and, C. Tiberius; , "A low-complexity UWB receiver concept for TOA based indoor ranging," *IEEE International Conference on Ultra-Wideband,* (ICUWB 2009) , vol., no., 9-11 Sept. 2009, pp. 618-623.

[15] D. Dardari, A. Conti, U. Ferner, A. Giorgetti, and M. Win, “Ranging with ultrawide-bandwidth signals in multipath environments,” *Proceedings of the IEEE*, vol. 97, no. 2, pp. 404 –426, Feb. 2009

[16] D. Wu, L. Bao, and, R. Li, “UWB-based localization in wireless sensor networks”, *Int. J. Commun. Network Syst. Sci.* 2009, 2, 407-421.

[17] Yung-Hoon Jo, Joon-Yong Lee, Dong-Heon Ha, and, Shin-Hoo Kang, "Accuracy Enhancement for UWB Indoor Positioning Using Ray Tracing," *Position, Location, And Navigation Symposium*, 2006 IEEE/ION , pp. 565−568, April 25-27, 2006.

[18] Z. Sahinoglu, S. Gezici, and I. Guvenc, *Ultra-Wideband Positioning Systems: Theoretical Limits, Ranging Algorithms, and Protocols,* Ca*m*bridge University Press, 2008.

[19] G. Bellusci, G. J. M. Janssen, Junlin Yan, and, C. C. J. M Tiberius, "Low complexity ultra-wideband ranging in indoor multipath environments," *Position, Location and Navigation Symposium*, 2008 IEEE/ION , pp. 394−401, 5−8 May 2008.

[20] L. Mucchi, P. Marcocci, "A new parameter for UWB indoor channel profile identification," *IEEE Transactions on Wireless Communications,* vol. 8, no. 4, pp.1597−1602, April 2009.

[21] I. Guvenc, Chia-Chin Chong, F. Watanabe, "NLOS Identification and Mitigation for UWB Localization Systems," *IEEE Wireless Communications and Networking Conference*, (WCNC 2007). , pp.1571−1576, 11−15 March 2007

[22] S. Maranò, W. M, Gifford, H. Wymeersch, M. Z. Win, "NLOS identification and mitigation for localization based on UWB experimental data," *IEEE Journal on Selected Areas in Communications*, vol. 28, no. 7, pp. 1026−1035, September 2010

[23] Bill Rison, “Time of Arrival Location technique,” Internet: http://www.ee.nmt.edu/~rison/ee389_spr08/toa.pdf, Spring 2008, [Jan. 29, 2011]

[24] Zhenzhen Ye, Chunjie Duan, P. V. Orlik; Jinyun Zhang, A. A. Abouzeid, "A Synchronization Design for UWB-Based Wireless Multimedia Systems," *IEEE Transactions on Broadcasting*, vol. 56, no. 2, pp.211–225, June 2010

[25] Chiara Falsi, Davide Dardari, Lorenzo Mucchi, and Moe Z. Win, “Time of arrival estimation for UWB localizers in realistic environments” *EURASIP J. Appl. Signal Process*ing, 2006 (January 2006)

[26] I. Guven, Chia-Chin Chong, Fujio Watanabe, and Hiroshi Inamura. 2008, “ NLOS identification and weighted least-squares localization for UWB systems using multipath channel statistics,” *EURASIP J. Adv. Signal Processing* 2008,

[27] M. Heidari, F. O Akgul, K. Pahlavan, "Identification of the Absence of Direct Path in Indoor Localization Systems," *IEEE 18th International Symposium on Personal, Indoor and Mobile Radio Communications*, (PIMRC 2007), pp.1–6, 3–7 Sept. 2007

[28] Camillo Gentile, “UWB-MIMO Channel Propagation Measurment in the 2-8GHz Spectrum,” Internet: http://www-x.antd.nist.gov/uwb/, [Jan. 21, 2009]

[29] C. Gentile, A.J.Braga, A.Kik, "A Comprehensive Evaluation of Joint Range and Angle Estimation in Ultra-Wideband Location Systems for Indoors," Communications, 2008. ICC ’08. *IEEE International Conference on* , vol., no., pp.4219-4225, 19-23 May 2008

[30] Tom Germano, “Wavelets in Multiresolution Analysis,” Internet: http://davis.wpi.edu/~matt/courses/wavelets/, [Feb. 15, 1999]

[31] Zhan Xu, Jianping An, Kai Yang, Xiangyuan Bu, Peng Liu, "Rapid and Low-Complexity Synchronization for IR-UWB Receiver," 4th *International Conference on Wireless Communications, Networking and Mobile Computing,* (WiCOM '08) pp.1−5, 12−14 Oct. 2008

[32] M. Di Renzo, L.A.Annoni, F. Graziosi, F. Santucci, "A Novel Class of Algorithms for Timing Acquisition of Differential Transmitted Reference UWB Receivers: Architecture, Performance Analysis and System Design," *IEEE Transactions* on *Wireless Communications*, vol. 7, no. 6, pp. 2368−2387, June 2008

[33] S. Maranò, W. M. Gifford, H. Wymeersch, and M. Z. Win, "NLOS identification and mitigation for localization based on UWB experimental data," *IEEE Journal on Selected Areas in Communications*, vol. 28, no. 7, pp. 1026 –1035, sep. 2010

[34] L. Mucchi, P. Marcocci, "A new parameter for UWB indoor channel profile identification," *IEEE Transactions on Wireless Communications*, vol. 8, no. 4, pp.1597−1602, April 2009

[35] I. Guvenc, Z. Sahinoglu, "Threshold selection for UWB TOA estimation based on kurtosis analysis," *IEEE Communications Letters,* vol. 9, no. 12, pp. 1025- 1027, Dec. 2005

[36] Khodjaev, Jasurbek Park, Yongwan Choi, Jeonghee "A novel UWB channel identification parameter for indoor positioning applications", *Annals of telecommunications - annales*

[37] I. Guvenc and Z. Sahinoglu, "Threshold-based TOA estimation for impulse radio UWB systems," *in Proc. IEEE Int. Conf. on UWB,* Zurich, Switzerland, Sept. 2005, pp. 420–425.

[38] Chi Xu, C.L Law, "Delay-Dependent Threshold Selection for UWB TOA Estimation," *IEEE Communications Letters,* vol. 12, no. 5, pp. 380−382, May 2008

[39] I. Guvenc, Z. Sahinoglu, "TOA estimation with different IR-UWB transceiver types," *IEEE International Conference on Ultra-Wideband,* (ICU 2005), pp. 426–431, 5−8 Sept. 2005

[40] Liu, T. C. Dong and X. Lu, “Multiresolution wavelet de-noising for ultra-wideband time-of-arrival estimation with regularized least squares,” *Physical communication* 2009, vol. 2; no. 4, page 285−295

[41] John M. O’ Toole,“Accurate and Efficient Implementation of the Time and Frequency Matched Filter”, *The University of Queensland*

[42] D. Donoho and J. Johnstone, “Ideal spatial adaptation by wavelet shrinkage,” *Biometrika* 81 (3) (1994), pp. 425–455.

[43] D. Donoho, “de-noising by soft-thresholding,” *IEEE Trans. Inf. Theory* 41 (3) (1995), pp. 613–627

[44] B. Vidakovic, “Wavelets and Bayesian statistics,” *Interface*’94, 1994 pp. 15–18.

[45] D. B. Percival and A. T. Walden, “Wavelet methods for time series analysis.” *Cambridge ; New York: Cambridge University Press,* 2000.

[46] A. Mertins, Signal analysis *wavelets, filter banks, time-frequency transforms, and applications,* English rev. ed. Chichester, West Sussex, England, *New York: J. Wiley*, 1999

[47] S. G. Mallet, “A theory for multiresolution signal decomposition: The wavelet representation,” *IEEE Trans. Pattern Anal. Mach. Intel.*, 1989, 11(7), 674-93

[48] I. Shim, J. J. Soraghan, and W. H. Siew, "Detection of PD utilizing digital signal processing methods. Part 3: Open-loop noise reduction," 2001

[49] Z. Zhao, M. S. Demokan, and J. M. K. MacAlpine, “Optical fiber acoustic sensor for sensing and locating partial discharges in high voltage oil-filled power transformers, ” *IREE* Soc 1996 p. 286-9 Milsons Point NSW Australia, 1997

[50] I. Sharp, K. Yu,Y.J. Guo, "Peak and leading edge detection for time-of-arrival estimation in band-limited positioning systems," *IET Communications,* vol. 3, no. 10, pp. 1616–1627, October 2009

[51] Tsai, Shu-Jen Steven, *Power Transformer Partial Discharge (PD) Acoustic Signal Detection using Fiber Sensors and Wavelet Analysis, Modeling, and Simulation,* Master thesis, 2006

[52] Sjoerd Op ’t Land, *Ranging and Localization error in mitigation in indoor obstructed direct path conditions,* (Msc thesis), University of Twente, 2010.

[53] X. Ma, C. Zhou, and I. J. Kemp, "Automated wavelet selection and thresholding for PD detection," 2002.

[54] I. Guvenc, Chia-Chin Chong, F. Watanabe, "NLOS Identification and Mitigation for UWB Localization Systems," *Wireless Communications and IEEE Networking Conference*, (WCNC 2007), pp. 1571–1576, 11-15 March 2007.

[55] İsmail Güvenç, Chia-Chin Chong, Fujio Watanabe, and Hiroshi Inamura, “NLOS Identification and Weighted Least-Squares Localization for UWB Systems Using Multipath Channel Statistics,” *EURASIP Journal on Advances in Signal Processing, vol.* 2008.

[56] J. Khodjaev, Y. Park, "A novel UWB channel identification parameter for indoor positioning applications." *Annals of Telecommunications*

[57] J. A. K. Suykens, T. Van Gestel, J. De Brabanter, B. De Moor, J. Vandewalle, “Least Squares Support Vector Machines,” *World Scientific, to appear.*

[58] Kristiaan Pelckmans, Johan A. K. Suykens. ”LS-SVMlab: a MATLAB/C toolbox for Least Squares Support Vector Machines”

[59] J.A.K. Suykens, T. Van Gestel, J. De Brabanter, B. De Moor, J. Vandewalle, “Least Squares Support Vector Machines,” *World Scientific, to appear.*

[60] N. Cristianini, J. Shawe-Taylor, *An Introduction to Support Vector Machines, C*ambridge University Press, 2000.

[61] B. Sch¨olkopf, C. Burges, A. Smola, *Advances in Kernel Methods - Support Vector Learning*, MIT Press, 1998.

[62] B. Sch¨olkopf, A. Smola, *Learning with Kernels*, MIT Press, Cambridge MA, 2002.

[63] Jieping Ye, Tao Xion, “SVM versus Least Squares SVM,” *Eleventh International Conference on Artificial Intelligence and Statistics, 2007*

[64] F. Montorsi, F. Pancaldi, G. M. Vitetta, "Statistical characterization and mitigation of NLOS errors in UWB localization systems," *IEEE International Conference on Ultra-Wideband (ICUWB 2011)* pp. 86−90, 14-16 Sept. 2011

[65] Kristiaan Pelckmans and Johan Suykenshttp, “Least Square Support Vector Machine,” Internet: http://www.esat.kuleuven.be/sista/lssvmlab/, [Nov. 4,2011]

[66] I. Guvenc, C. C. Chong, and F. Watanabe, “ Analysis of a Linear Least-Squares Localization Technique in LOS and NLOS environments,” *in Proc. IEEE Veh. Technol. Conf. (VTC), Dublin, Ireland,* pp. 1886−1890, April 2007.